The Exploration and Application of Nuclear Magnetic Resonance (NMR): An investigation into the compound $KMnO_4$ (Potassium Permanganate)

by

EMMET WISE

A THESIS

Presented to the Department of Physics
and the Robert D. Clark Honors College
in partial fulfillment of the requirements for the degree of
Bachelor of Science

December 2019

An Abstract of the Thesis of

Emmet for the degree of Bachelor of Science
in the Department of Physics to be taken December 2019

Title: The Exploration and Application of Nuclear Magnetic Resonance (NMR): An investigation into the compound $KMnO_4$ (Potassium Permanganate)

Approved: _____*Bryan Boggs, Ph.D*_____
Primary Thesis Advisor

Examining compounds through nuclear magnetic resonance spectroscopy allows scientific researchers to better understand the materials being used in not only a scientific setting, but in everyday life as well. One such compound that is analyzable through NMR is potassium permanganate, also known as $KMnO_4$. This compound, while researched in other professional projects, is somewhat lacking in information due to many of these studies having occurred during the 1960s and 1970s, before the widespread use of computing. The theory would suggest that, by incrementally increasing the concentration of $KMnO_4$ dissolved in a deionized water solution, the coupling between the protons in the compound to each other and the environment to increase. This increase in coupling indicates that the height of the resonance peak will increase then decrease and the width of the resonance peak will more gradually increase. The results derived from this research project suggest that this is the case.

Acknowledgements

I would like to take this time to thank Professor Bryan Boggs, Professor James Schombert, and Professor Samantha Hopkins for acting as my thesis committee, as well as providing support as I wrote my thesis. I am honored by having such amazing professors guide me through the process of writing a thesis and my gratitude is immeasurable. I should also thank advisors such as Professor Fisher of the department of physics and Ms. Miriam Jordan of the Clark Honors College for providing so much help for not only my thesis but determining my path through college as a whole. Finally, I would like to thank my parents for always being supportive of my studies and for always believing in my academic abilities.

Table of Contents

List of Figures

List of Tables

Introduction/Background Information:

Within the field of physics, there are many ways that one can analyze a compound to better understand its properties and how it functions when interacting with other materials. One of the various methods employed by scientists today is the method of nuclear magnetic resonance spectroscopy. Before further explaining what NMR spectroscopy is, it is prudent to explain some fundamental facts and properties regarding atoms and how the application of a magnetic field can affect said atoms. All atoms have a nucleus as a center and contained within said nucleus are nucleons. These nucleons, which are also referred to as protons or neutrons, have a spin and magnetic moment, which causes them to act in a manner similar to that of small magnets. With this established, one may now discuss how the application of a magnetic field and the measurement of the effect said field has on the substance being analyzed can give information about the material.

NMR, or Nuclear Magnetic Resonance, has a long history of study, beginning primarily in the 1940s through two separate researchers, Felix Bloch and Edward Mills Purcell. Their work led to the moment in 1952, where “the Nobel Prize for physics was awarded to Felix Bloch and M. Purcell. In his Nobel lecture, 11 December, 1952, entitled ‘Research in nuclear magnetism’ Purcell already described all basic quantities and processes controlling NMR spectra” (Pfeifer 155). With the basics of nuclear magnetic resonance established, later developments went into application. One example of this development in application came in the years following Bloch and Purcell as “Organic Chemists soon found that NMR spectroscopy was an ideal technique for elucidating or verifying the structure of moderate sized molecules” (Becker 297). Since

then NMR has commonly been used as a means of studying both organic and non-organic compounds to obtain information not available through previous forms of study. This development of NMR has continued into the modern day and various forms of NMR are still used in labs across the world today.

With the introduction to this thesis and history of NMR put forth, it now seems prudent to talk about what this paper seeks to accomplish. $KMnO_4$, also known as potassium permanganate, is a compound with a well-documented history in NMR research. Some examples of past studies which employed the compound include determining "the chemical shift of $^{55}MnO_4$ in several solvents and in mixtures of water and acetone" (Gudlin 268), as well as finding "The quadrupole coupling constant and the electric field gradient asymmetry parameter n/… determined directly from the satellites of the dispersive mode NMR lineshape for the ^{55}Mn resonance in polycrystalline $KMnO_4$" (Wadsworth 424). In contrast to these studies, this thesis focuses less on variations in solvents or quadrupole coupling, and more of the process of nuclear magnetic resonance itself and how concentration of $KMnO_4$ can affect the height and width of the observed resonance peak. In theory, the addition of $KMnO_4$ increases the coupling of the protons to their material environment through dipole-dipole interactions. The addition of $KMnO_4$ also, in theory, increases coupling of protons to other adjacent protons. Together, these two interactions should lead to an increase and then decrease in the height of the measured resonance peak and a general increase in the width of the resonance peak overall. This proton to environment and proton to proton coupling will be discussed in much finer detail in the subsequent sections of this paper, further describing how such interactions occur and why. The data

presented following this expanded discussion in this thesis will demonstrate this to be true, using multiple graphs to convey the effect that varying concentrations of $KMnO_4$ can have on nuclear magnetic resonance. It should also be noted that, in regard to the experiments in this thesis, all tests were conducted using a continuous-wave, or CW, NMR system. In a CW NMR spectrometer "the compound is irradiated with electromagnetic energy of a constant frequency while magnetic field strength is varied or swept… by this technique the protons are brought into resonance one by one" (Balti 22). While other forms of NMR spectroscopy exist, continuous-wave was the primary means of spectroscopy available given the materials supplied.

Now, one may question why this thesis itself is important to the field, as well as why the field of nuclear magnetic resonance spectroscopy is important or significant today. To answer the first question, one need only look at one example of NMR research that has been performed on the compound $KMnO_4$ in the past. This example, dated November 1968, discusses "two cases for which spin-spin coupling with ^{17}O was determined. The first concerns J (^{55}Mn – ^{17}O) in. MnO4-. Here the ^{17}O nmr spectrum exhibits the effect of quadrupole relaxation by ^{55}Mn" (Broze 1600). This article, along with other similarly dated research pieces, make up much of the current understanding of the compound $KMnO_4$. These dates then indicate that said research was done when computation was not as accessible and thus learning more about the compound with modern technology could be beneficial for future research in the field of NMR. To answer the second question, one must look to a much more recent example of NMR research, that being this article about introducing "a new class of pure shift experiments (PSYCHE) with superior sensitivity spectral purity, and tolerance of strong coupling"

(Foroozandeh 6990). This paper, published May 2014, demonstrates that even today the field of NMR spectroscopy is active, as gaining knowledge about the compounds and materials that make up many of the objects we use today is essential.

Resonance Condition

The first matter to discuss is the subject of the resonance condition. To understand this, one must first consider a nucleus consisting of nucleons placed within a steady magnetic field $H_{0,}$ from now on referred to as the longitudinal field. The nucleus possesses a spin with spin number I > 0, meaning that it has a magnetic moment μ. Due to this magnetic moment and spin number I > 0, the nucleus will possess energy states corresponding to the measurable values of angular momentum in units of $\hbar$. In the case of spin number, I = 1/2, this creates two energy states, referred to for the sake of this discussion as the low energy state and high energy state. When the spin system lacks a form of applied energy such as the magnetic field, said spin system should be nearly exclusively in the lower energy state. The energy of the magnetic moment E is equal to the dot product of the magnetic moment and the longitudinal magnetic field, $E = -\vec{\mu} * \vec{H_0}$. This understanding proves important, as should the applied RF energy be resonant, it can allow for some nucleons to absorb said energy and transition from being parallel to the longitudinal magnetic field, the low energy state, to being antiparallel, the high energy state. With this model in mind, one should now consider the model presented in the image included below. This model demonstrates a magnetic dipole placed in the steady longitudinal magnetic field precessing around the direction of the longitudinal magnetic field. The rate of this precession is given by the Larmor

frequency, $\omega_0 = \gamma * H_0$, with γ being the gyromagnetic ratio. This "frequency of precession (also called the Larmour frequency, abbreviated v_L) is simply the number of times per second that the proton precesses in a complete circle. A proton's precessional increases with the strength of B_0" (Soderberg 237). To clarify further, the B_0 referenced in the previous quote is also known as magnetic flux density, while the H_0 stated in the Larmor frequency equation is also known as magnetic field strength. The relationship between the two similar magnetic field values is best represented in the equation $B = \mu_m*H = (\mu_0*K_m)*H$, μ_0 being the magnetic permeability and K_m being the relative permeability of the material. Now one must consider the application of another field placed perpendicular to the steady longitudinal field, now classified as the transverse field. This transverse field will cause the magnetic dipole μ to increase the angle between it and the direction of the longitudinal field, thus increasing the energy of the dipole. Should the transverse field be set to rotate about the axis of the longitudinal field at the Larmor frequency alongside the magnetic dipole, then the transverse field will cause the angle and thus the energy of the nucleon to increase. This increase in the nucleon's energy eventually allows it to reach a higher energy state, as described in the initial model, and thus allow resonance to occur (Andrew 7-11).

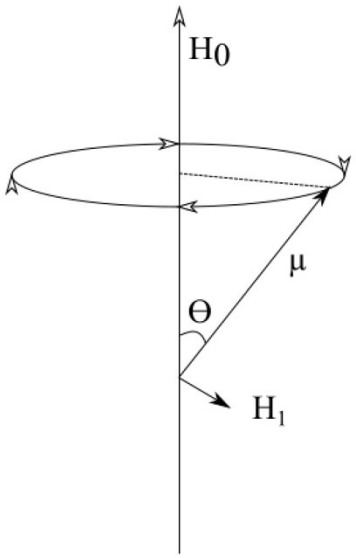

Fig. 1: Classical Larmor Precession of a magnetic moment μ in a magnetic field H_0, as illustrated in Andrew's book

Spin Lattice Interaction and Relaxation Time T_1

Now that this transition in energy levels is understood in its most fundamental form, one can now begin to understand the process of transition on a larger scale and the process that creates relaxation time. As Callaghan makes clear, "the free precession of nuclear spins does not continue indefinitely. Ultimately, the off-diagonal elements of the density matrix lose phase coherence while the diagonal elements gradually return to their thermal equilibrium state, two processes known, respectively, as T_2 (spin-spin) and T_1 (spin-lattice)" (Callaghan 595). This thesis will first explain relaxation time T_1, beginning by considering a group of the same atomic nuclei with 1/2-spin within a steady longitudinal magnetic field, H_0. Next, one must assume that there is only a weak coupling existing between nuclear spins, as this allows the magnetic interaction between nuclei to be ignored to a first approximation, thus allowing the model to treat each

separate nuclei in the group the same as the nuclei modeled in the previous section. As established in the previous section, when a transverse magnetic field set to the resonant frequency is placed perpendicular to the longitudinal magnetic field, the energy levels of the nucleons will begin to change. By the theorem of Einstein Coefficients, there is an equal probability for transition into a higher energy state through absorption as there is transition into a lower energy state through stimulated emission. If the number of nuclei in each of the two energy levels were equal, then the average rate of transition to the higher energy level and the lower energy level would be equal, however, due to the nuclear spins being at equilibrium at the temperature T_s, the number of nucleons in the lower energy level exceeds the number of nucleons in the higher energy level by the Boltzmann factor. Due to this excess number of nucleons in the lower energy state, this results in a net energy absorption due to the Radiofrequency field, which then leads to some of the nucleons transferring from the lower energy state to the higher energy state (Andrew 11-16).

With this system established, now one must consider the issue of the lattice, that being the substance that the nuclear magnets are affixed in. In an ideal system, in which there is no lattice-spin interaction, the additional nucleons in the lower energy state decreases, thus implying that the spin temperature T_s increases gradually through RF heating. However, in a physical system that would be observed within an experiment, the lattice in some small way does affect the nuclear spins, leading to spin and lattice coming to thermal equilibrium at the same temperature, this temperature usually being very close to the lattice temperature T. This is significant as this indicates that while radiation produced by the RF causes some of the excess nucleons to shift from the

lower energy level to the higher energy level, the interaction with the lattice causes some of these same nucleons to return to the lower energy level. This process in which the spin and lattice approaches thermal equilibrium is often referred to a thermal relaxation process and leads to the term T_1 which represents the spin relaxation time, $T_1 = \frac{1}{2W}$, W being the average transition rate between the upward transition and downward transition (Andrew 11-16).

Spin-Spin Interaction and Relaxation Time T_2

The next step in understanding the basic theory behind NMR, now that spin-lattice relaxation time has been covered, is spin-spin relaxation. The basic concept focuses on the idea that since each nucleus contains a magnet dipole moment and multiple atoms/nuclei will be within a sample/substance, then the various nuclei's magnet dipole will interact. This interaction involves each nucleus suffering effects from both the steady field H_0, and the adjacent local magnetic fields produced by neighboring nuclei, H_{loc}. Due to the existence of this local magnetic field affecting each nucleus uniquely, each total magnetic field $H_{tot} = H_0 + H_{loc}$ will be slightly different for each nucleus, meaning the resonance condition will not be sharp, but rather each energy level will be broadened by an amount of order $g * \mu_0 * H_{loc}$, μ_0 being the magnetic dipole moment of one nucleus and g representing the g-factor. This broadening process is often referred to as inhomogeneous broadening and can have a significant effect on results of the experiment (Andrew 16-18).

Along with being affected by the neighboring magnetic fields, there is another physical mechanism at play that can affect the magnetic field of a nucleus. This other physical phenomenon occurs when a spin precessing about H_0, producing a Larmor frequency oscillating magnetic field, produces said oscillating field at another spin's position. This production of an oscillating field at another spin's position can cause a transition in this second spin, and in doing so there is a mutual exchange in energy through this interaction. This energy exchange between the two spins further broadens the resonance by an amount of the order of H_{loc}. These two processes which broaden the resonance lead to the creation of T_2, which represents the phase-memory time constant of a spin-spin interaction, much in the same way as T_1 does for the spin-lattice. It is due to this similarity that T_1 is referred as the longitudinal relaxation time while T_2 is referred to as the transverse relaxation time. While there are multiple definitions of T_2 as a number, the most concrete is $T_2 = \frac{g(\nu)_{max}}{2}$, $g(\nu)_{max}$ being the maximum value of the line-shape function as a function of frequency ν (Andrew 16-18).

Saturation

With the spin-lattice relaxation time T_1 and the phase-memory time constant T_2 properly defined and understood, one may now discuss the steady-state behavior of a spin-lattice system placed within an applied transverse magnetic field. When there is no transverse magnetic field, one calculates the time variation of n, the excess nuclei in the lower energy state, as $\frac{dn}{dt} = \frac{(n_0 - n)}{T_1}$, n_0 being the excess number of nuclei in the

lower state when the spin system and the lattice are in thermal equilibrium. In the case where $T_s > T$, that being when n is negative, this would then indicate that $\frac{dn}{dt}$ is greater than zero and thus the excess nuclei in the lower energy state increases over the time period T_1. In the event that there is a transverse magnetic field, this changes the equation to $\frac{dn}{dt} = \frac{n_0 - n}{T_1} - 2nP$, P being the probability per unit time that a nuclei transitions to a higher energy level. The steady state is reached when $\frac{dn}{dt} = 0$, meaning that a steady state value for n, n_s, can be defined through the following equation:

$\frac{n_s}{n_0} = \frac{1}{1 + 2PT_1}$. This equation for the number of nuclei at the steady state indicates that n_s decreases when P or T_1 increases and increases when P or T_1 decreases. It can be shown that the probability P can be stated as $P = \frac{1}{4} * \gamma^2 * H_1^2 * g(\nu)$, indicating then that $\frac{n_s}{n_0} = [1 + \frac{1}{2} * \gamma^2 * H_1^2 * T_1 * g(\nu)]^{(-1)}$, which can then act as the definition of the saturation factor Z. This saturation factor is then applicable in demonstrating the relation between the lattice temperature T and the spin temperature T_s, at the steady state, through this simple equation, $T_s = \frac{T}{Z}$ (Andrew 18-21).

Apparatus:

With some theory behind nuclear magnetic resonance spectroscopy firmly established in the preceding section, one may now discuss the specifications and details regarding the NMR system used in this thesis project, a Continuous-Wave NMR system constructed and maintained in the Advanced Projects Lab of the University of Oregon Department of Physics. While this system existed in a more basic form before this thesis project began, the research process required the system to be modified and upgraded using some of the devices which will be discussed later in this section. To begin describing the apparatus, it seems prudent to compose a list detailing all of the equipment used in the construction of this system, included below:

- RIGOL DG 4162 Function/Arbitrary Waveform Generator (2 Channel)
    - 160 MHz
    - 500 MSa/a
- Custom Bridged-T Circuit (constructed specifically for NMR system)
- RIGOL DP1308A Programmable DC Power Supply
- Custom Magnetic Field Controller (constructed specifically for NMR system)
- Electronic Measurement Inc. TCR Power Supply
- EG&G Princeton Applied Research Model 5202 Lock-In Amplifier 0.1-50MHz
- RIGOL DG1022 Function/Arbitrary Waveform Generator (2 Channel)
    - 20MHz
    - 100 MSa/s
- Tektronix DPO Digital Phosphor Oscilloscope
    - 3.5 GHz

- 40 GS/s

- Magnet System (constructed specifically for NMR system)
- FLUKE 8845A 6 ½ Digit Precision Multimeter
- Stanford Research systems Model SR445 DC-300 RF MHz Amplifier
- Integrated water-based cooling system

Also included is a block diagram of the NMR that demonstrates the connections between the components that make up the NMR system:

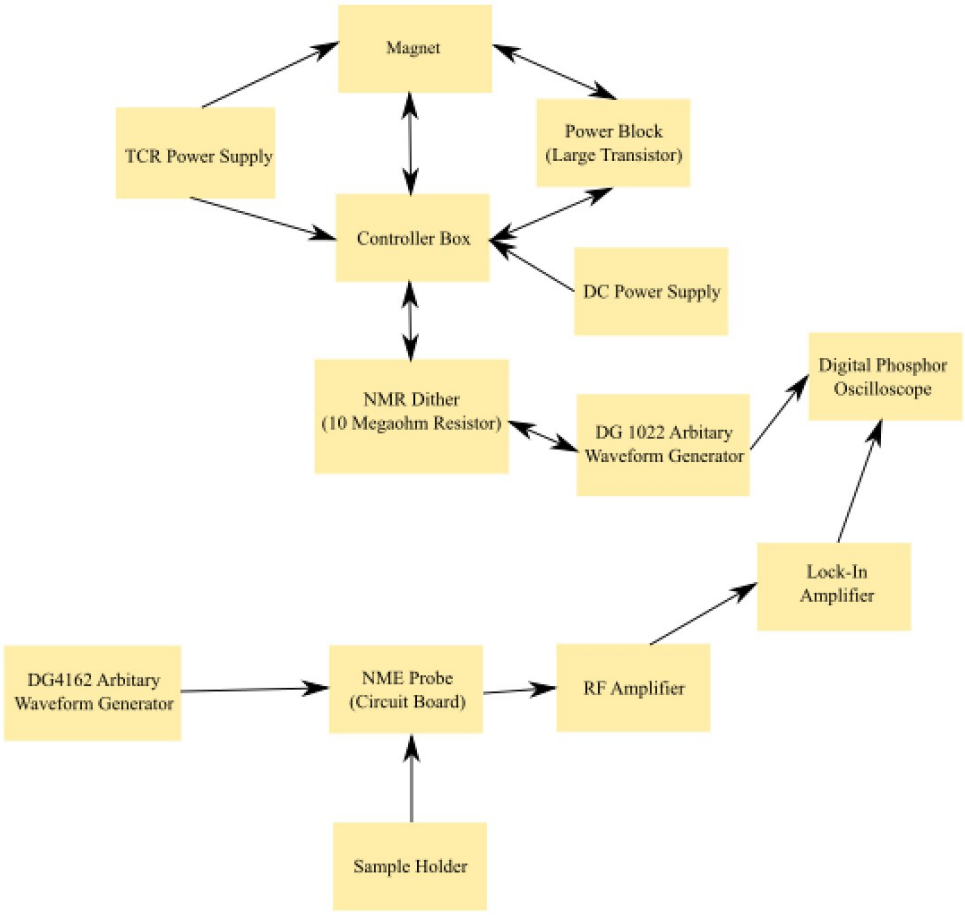

Fig. 2: block diagram demonstrating connections between components that make up NMR system

Each piece of equipment plays a key role in the operation of the NMR system and its use on the samples studied in this research project. The DG 4162 waveform generator, henceforth referred to as waveform generator #1, connects directly to the input of the custom Bridged-T circuit using coaxial cables with BNC connectors. The output of this Bridged-T circuit then flows through the DC-300 RF amplifier and then connects to the signal input of the Lock-In Amplifier. The Lock-In Amplifier is one of the most crucial pieces of the system, as it provides both the in-phase and in-quadrature components of the signal which will be analyzed to find the resonance. These in-phase and in-quadrature outputs that the Lock-In Amplifier provides then connect to the Channel 1 and Channel 2 inputs on the Tektronix Digital Phosphor Oscilloscope, which unlike many other oscilloscopes contains a fully functioning computer. The reason these two components of the signal connect to these two channels on the oscilloscope is because once the oscilloscope computer is turned on and the Tekscope program on the oscilloscope computer begins to run, the program can then depict these two components of the signal in a visual manner that allows one to find the resonance peak for any samples placed within the designated area of the magnet, the sample holder.

Another key factor that makes up the overall NMR system is the means by which the system is powered. Within the system there are two primary power supplies, the DC power supply and the TCR power supply. The DC power supply, which provides the initial power voltage and current for the magnet system, with the voltage displayed on the FLUKE multimeter, connects directly into the custom controller box through a set of three wires. The controller box is the means by which the one performing the experiment using the NMR may alter the strength of the magnet's field,

through both the course field knob that handles larger changes in magnetic field, while the fine field knob is capable of altering said field by a smaller metric. The TCR power supply, which takes the initial strength of the magnet and increases it to a scale that is actually applicable to the function of the system, connects directly to the controller box as well as a component dubbed the power block, which in reality is just a high-power transistor on a piece of Teflon that connects to controller box and the magnet itself. The last few connections worth noting are how the corresponding sync for waveform generator #1 connects to the reference input on the Lock-In Amplifier, and how the DG 1022 Waveform Generator, henceforth referred to as waveform generator #2, has two connects. The first connection for waveform generator #2 is the one between it and the controller box, which runs through the NMR Dither, which consists of a 10 Megaohm resistor. The second connection simply connects the second waveform generator to Channel 3 on the oscilloscope computer, so that when Channels 1 and 2 are being displayed through the Tekscope program, one can see how the in-phase and quadrature components react when the dither is turned on and the magnetic field sweeps through a small range. To summarize, the power supplies, DC and TCR, provide the necessary power to allow the magnet to run, the amplifiers strengthen the output signal to the point where it can be observed through the oscilloscope, and the controller box provides the means by which one can control the field of the magnet and thus find the nuclear magnetic resonance for a substance.

Bridged-T Circuit

With the primary components of the NMR system properly summarized for the purposes of this research project, it now seems prudent to discuss the intricacies of the

Bridge-T circuit that allows the NMR system to function in its current form. To begin understanding such intricacies, one may first examine the images included below, which depict a simulation created ,using the open source software package known as QUCS (Quite Universal Circuit Simulator), of the Bridged-T circuit implemented, as

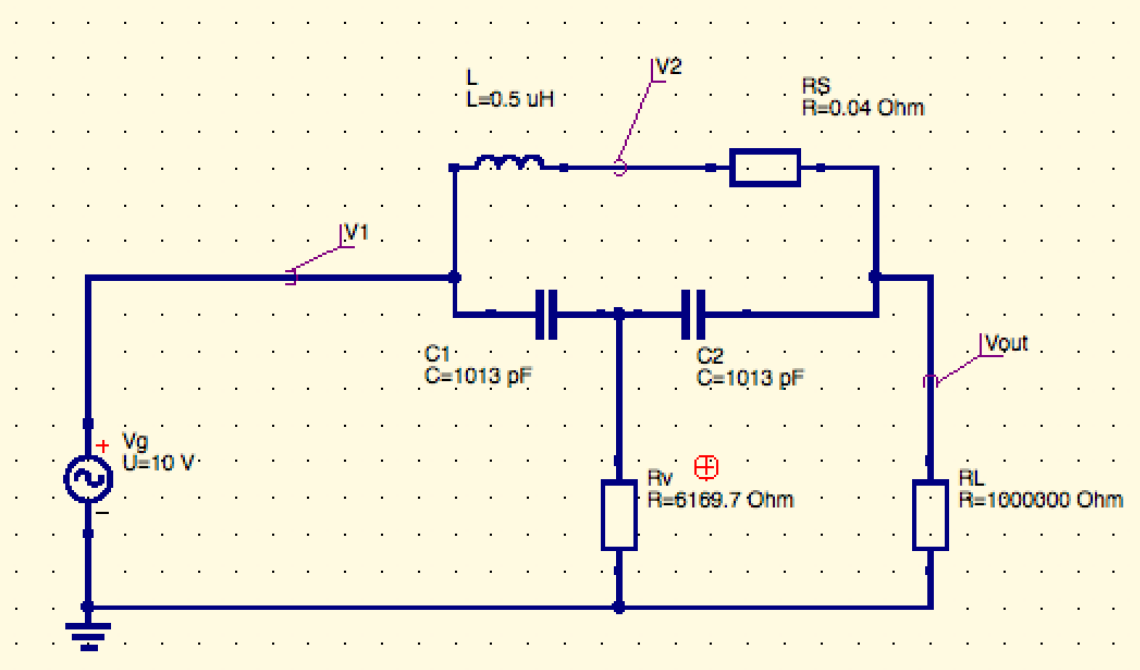

well as demonstrates the effect one produces when the resistance “Rv” on the bottom half of the circuit is changed:

Fig. 3: Bridged-T circuit used in NMR, created in QUCS

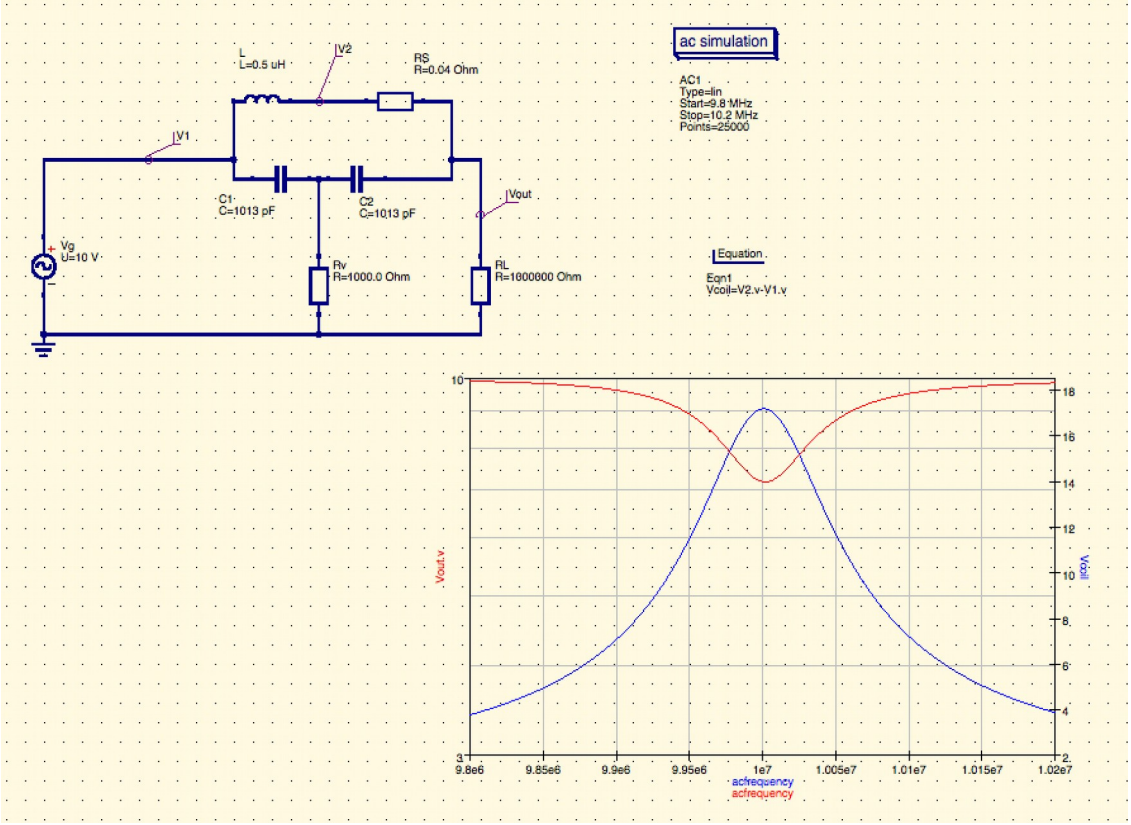

Fig. 4: Bridged-T circuit simulation run with Rv = 1000 ohms

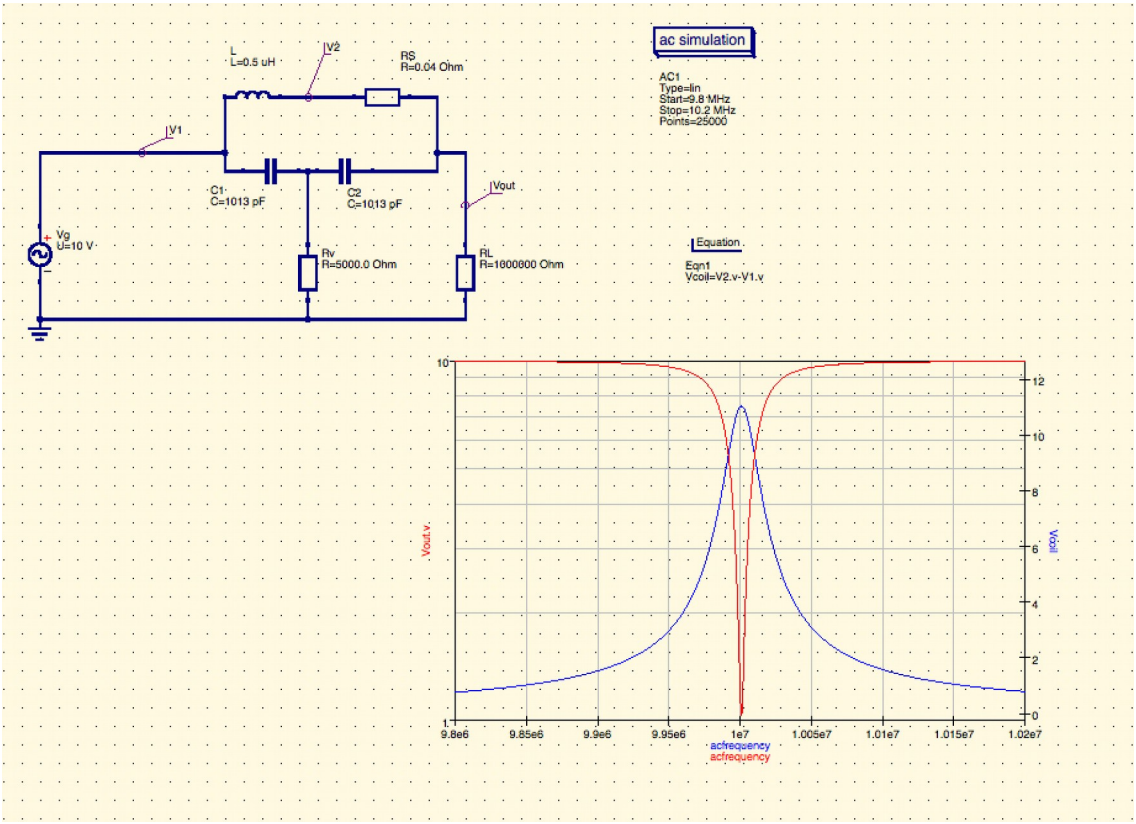

Fig. 5: Bridged-T circuit simulation run with Rv = 5000 ohms

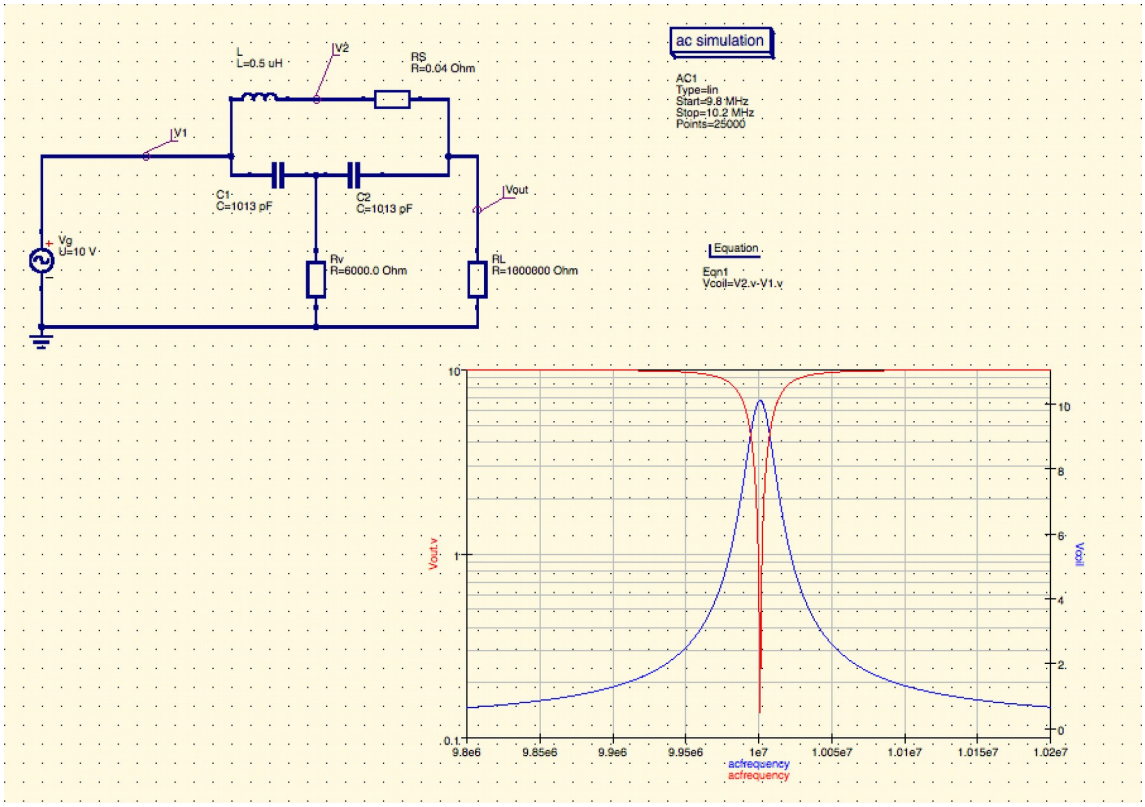

Fig. 6: Bridged-T circuit simulation run with Rv = 6000 ohms

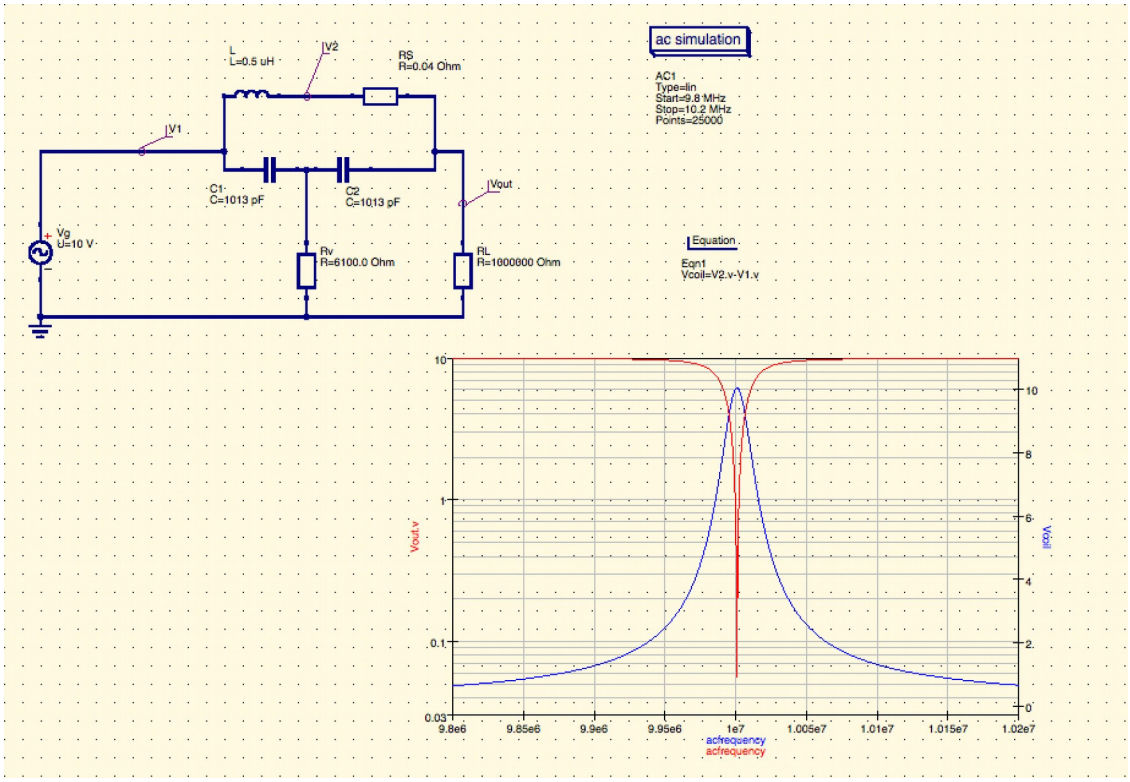

Fig. 7: Bridged-T circuit simulation run with Rv = 6100 ohms

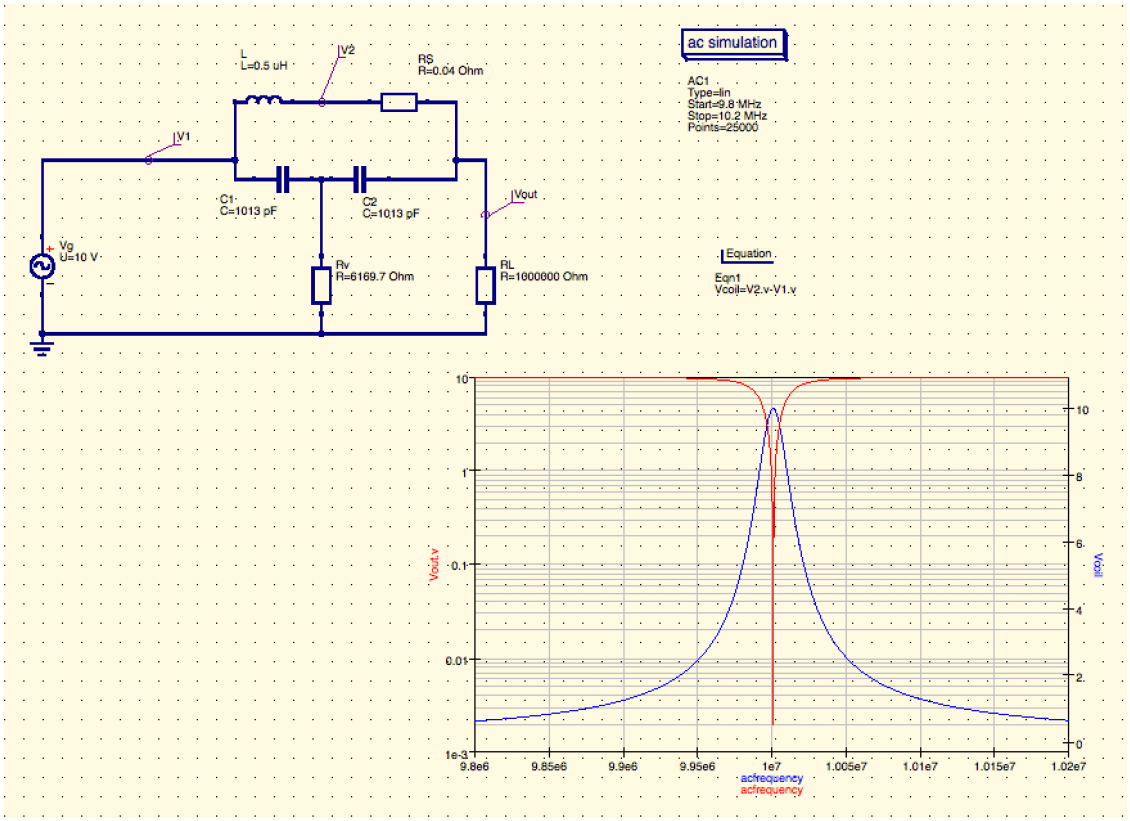

Fig. 8: Bridged-T circuit simulation run with Rv = 6169.7 ohms

To give context to the simulation, the device on the top half of the circuit labeled “L” represents the coil, that being a form of inductance, that wraps around the sample holder, with the “Rs” demonstrating the resistance inherent to the wire which the coil is made out of. Opposing this coil on the bottom half of the circuit is the two C’s, “C1” and “C2”, which refer to the two capacitors. These capacitors are intended to counteract or balance the reactance that is derived from the sample that would be placed inside the sample holder, which the coil on the top half of the circuit would go around. Underneath these capacitors is the resistance “Rv” which is supposed to act as an equalizing or balancing force to the resistance provided by the top half of the circuit, from both the coil itself as well as from the sample being tested, similar to the balancing of reactance that occurs through the capacitors. Once both reactance and resistance are properly balanced on each side of the circuit, one may be able to find the resonance, which is indicated through the simulation by the increasing peak of the coil voltage, V_{coil}, and the decreasing peak of the output voltage, V_{out}. This understanding is only furthered when one examines the changes that occurs through each of the simulation runs with different “Rv” values. As the “Rv” value gets closer to the ideal value, the sharper and deeper each respective V_{out} peak gets, thus indicating that the balanced signal being fed through the circuit is tiny and that the resonance is not difficult to observe when the resonance condition is reached. As the longitudinal field sweeps through the resonance, their follows a change in the sample’s absorption or resistance and dispersion or reactance. This change causes the circuit, being initially balanced, to become un-balanced, resulting in a change in the signal going through the circuit. This

change in the signal is then observed as the resonance peak displayed on the oscilloscope computer, thus indicating to the one operating the NMR system when the circuit becomes unbalanced. Multiple examples of this resonance peak are represented later in this research project, in the data and results section.

This understanding demonstrated in the simulation also aligns well with the information on Bridged-T circuit provided by Waring's article. As described in "A Bridged Tee Detector for Nuclear Magnetic Resonance" when discussing the general characteristics of a "Bridged Tee Circuit", "The applicable balance equations are

$$W^2 = 1/L * \frac{C_1 * C_2}{C_1 + C_2} \quad (1)$$

$$R = \frac{L}{C_1 + C_2} * r \quad (2)$$

The form of Eqs. (1) and (2) shows that two adjustments are necessary to balance the network. A convenient arrangement is to provide part of R and part of C variable. The circuit is then tunable for different input frequencies" (Waring 497). To give further context to this direct quote, the circuit that it refers to in the article is included in the image below:

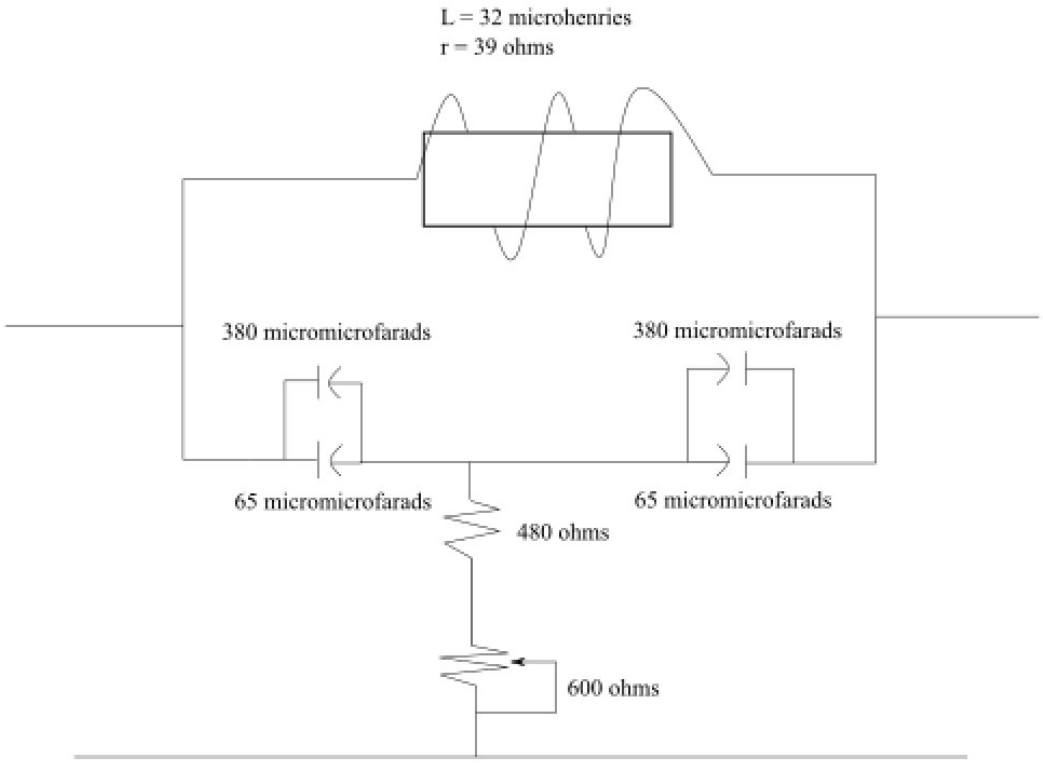

Fig. 9: Bridged-T circuit referenced in Waring article, recreated in Inkscape program

While there are some slight differences in the model provided in the article versus the circuit board displayed in the project's simulation, the basic structure is still predominantly the same, with "R" representing the resistors, and "C" representing the capacitors. Both models function under the fundamental principle that by providing a means of altering the values for the resistance and reactance, the NMR system can be tuned to detect the desired resonance peaks. To complete this understanding the bridged T circuit, one must finally examine the physical circuit implemented in the experimental NMR system used in this research project, as depicted in the images below:

Fig. 10: Top-down view of NMR Bridged-T circuit board inside aluminum casing

While it may not be clear from first glance, the physical circuit board implemented in this research project is nearly identical to the one depicted in the simulation, with one key difference. The gold tipped tubes present on each side of the circuit are the capacitors that make up two of the three primary components of the bottom half of the circuit. The wire running to the sample, as one may gather, is the coil with a certain reactance and resistance which one sees in the top half of the circuit. The previously mentioned key difference lies within the two blue boxes shown in the middle of the circuit, which represent the single resistance shown in the simulation. The reason for this difference is because these blue boxes are potentiometers, resistors whose resistances can be easily altered by tweaking its settings through the gold tip on each box. These potentiometers have a maximum resistance of 100 ohms and 10 kiloohms respectively, and by manipulating the value of each one can draw closer to the

resistance value necessary to balance the circuit, similar to the series of simulations demonstrated in the beginning of this section.

While applicable in many NMR studies, these types of bridge circuits have specific limitations that require the rest of the system to accommodate. This limitation is that Bridged-T circuits produce “mixed” types of signals, that being signals that include both the absorptive and dispersive component of the resonance. This mixture of the components means that instead of having a clear picture of either part of the resonance and the resulting resonance peak, it creates a mixed image. To accommodate for this issue, one must follow the method detailed in a later section of this thesis. This method explains that, through altering the input frequency from the primary waveform generator while the in-phase and in-quadrature components of the resonance are set to alternating current AC, one can separate the two components of the resonance, allowing someone to observe only one component at a time through the oscilloscope.

Sample Creation:

Along with the NMR apparatus that is operated to attain the data presented in this research project, another key part of the experiment is the creation and management of the $KMnO_4$ samples. To accomplish the primary goal of the project, that being demonstrating the change in the resonance based on the concentration of potassium permanganate, one requires a series of series of samples that presents a range of concentrations of the compound. To create this series of samples, one must first measure out various amounts of potassium permanganate in terms of grams, in the case of this project these amounts include 0.01g, 0.02g, 0.03g, 0.04g, 0.05g, 0.1g, 0.15g, 0.30g, 0.45g, 0.60g, 0.70g, 0.80g, 0.90g, 1.0g. Once these gram-based amounts of the

compound are properly measured, one then proceeds to dissolve each of these amounts into 100 milliliters of deionized water, mixing the solution until the formerly crystallized $KMnO_4$ is fully dissolved. Once fully dissolved, one can then measure out a volume of 150 microliters and place said volume in an appropriately sized test tube, repeating the process for each respective concentration and labeling them to indicate which concentration they are for future reference. Due to the progression that the project naturally followed, the actual labeling system employed is somewhat disorganized, with some samples being further down the alphabet but lower in concentration than others. With that in mind this project will simply refer to each sample by its amount of potassium permanganate in terms of grams, thus allowing said samples to demonstrate more easily the significance in resonance changes. It should also be mentioned that each of these test tubes is topped with a rubber stopper, limiting any contact with the air the sample may have and ensuring that minimal outside material can affect the results observed through the measurement process. Altogether, each sample is created through the same uniform and secure process, through which one can ensure there is little to no possible error caused through the preparation of the samples.

Sample Holder Creation

Along with the creation of the various samples necessary to perform the experiment described in this thesis project, the process also required the creation of a new component to ensure magnetic field homogeneity given the limited materials available, that being a new sample holder. This newly constructed component created for the purposes of this project primarily consists of three key parts. These parts are the

aluminum rod stand, the Teflon cylinder used to hold the sample tube, and the wiring which goes around the Teflon cylinder and connects to the circuit board, as pictured below:

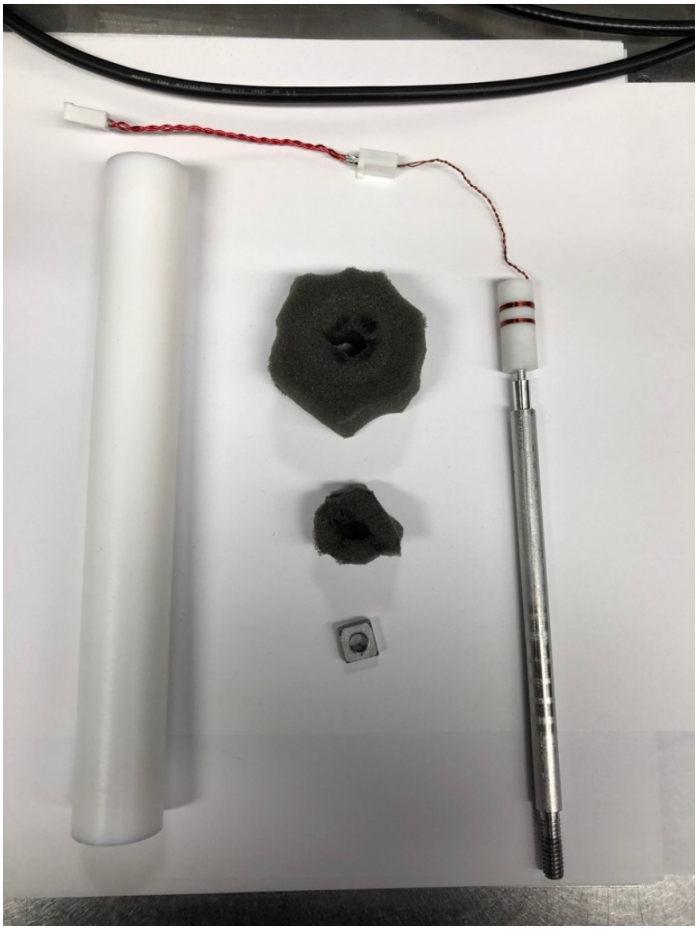

Fig. 11: (shown right) sample holder constructed from aluminum stand, Teflon cylinder, and wiring

The aluminum rod stand was constructed by cutting a length of an aluminum rod, and then threading both ends so that they take the form of a screw, thus allowing one end to screw into the holes on the table which the experimental NMR system rests on and the other to screw into the bottom of the Teflon cylinder. Excluding the screw-like ends, this placed the length of the stand at approximately 137.5 mm, thus placing the Teflon

cylinder that actually holds the sample tube at the approximate center in terms of distance and elevation between the two halves of the magnet, a point in space that should provide the greatest field homogeneity available for the experiment. In regard to the Teflon cylinder, the Teflon is primarily solid with one hole on each end of the cylinder, one threaded to allow for a screw and one set to hold the sample tube of a sample. The cylinder measures to 29.15 mm in length, with an outer diameter of 11.18 mm and an inner diameter of 6.4 mm, which allows for a sample tube with diameter 6.25 mm to fit tightly without making it difficult to swap with other sample tubes. Finally, wrapped around this Teflon cylinder is the 26-gauge wire, set into a series of grooves to reduce field inhomogeneity across any sample used and attaching to a 16-gauge wire extension to the two prong connectors on the bottom of the circuit board, as seen in the images below:

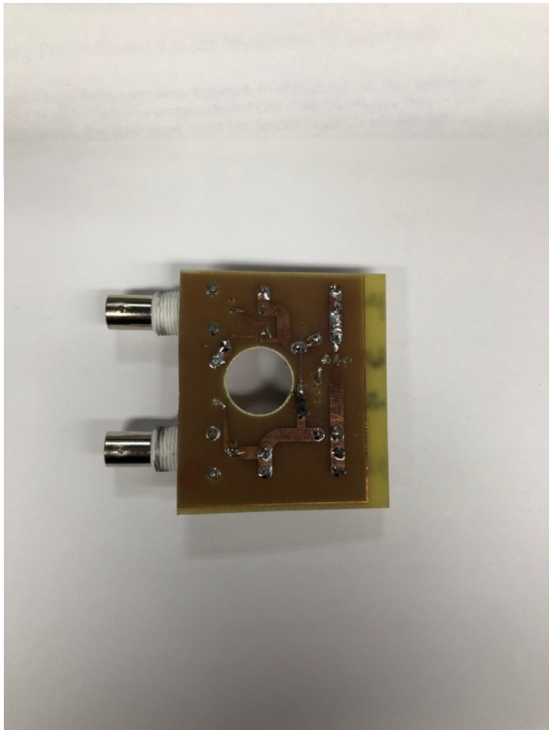

Fig. 12: Bottom side of NMR Bridged-T circuit board, demonstrating metal prongs that connect to wiring around sample holder

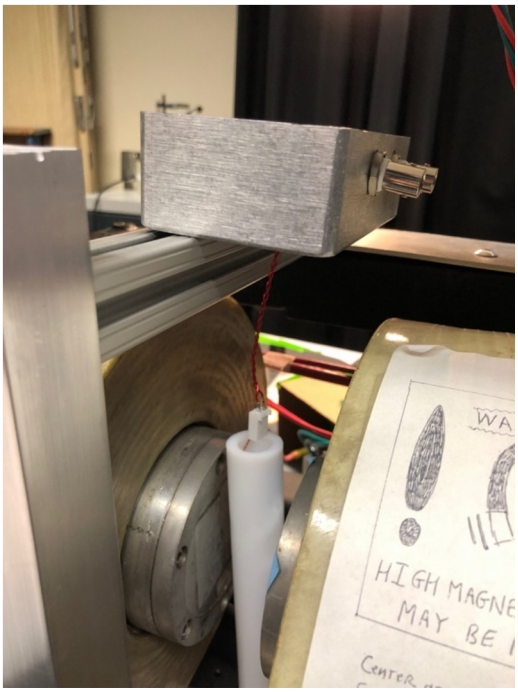

Fig. 13: Bridged-T circuit board as inside of the NMR system, illustrating how wiring connects to two prongs on bottom of circuit board

Temperature Shielding and Stability

With the creation of a new sample holder and the need to ensure the most accurate data possible, there arises the issue of providing temperature shielding and stability, guaranteeing that no fluctuations in the air or movement of the circuit board could affect any future research performed using the experimental system. This requirement leads to the creation of a new series of components that goes about providing this temperature shielding and physical stability. The first component for the temperature shielding comes in the form of a Teflon tube that encompasses the sample holder when the experimental NMR system is in use. This Teflon tube has a length of 203.2 mm, outer diameter of 26.1 mm, and an inner diameter of 15.2, meaning that is

can easily cover the Teflon cylinder in which the sample rests in, while still allowing for the sample holder as a whole to fit inside of it. To further the temperature shielding provided by this component, the Teflon tube is sealed using a piece of soft foam, which is cut into a circle and given a hole in the center, thus forming a ring that is then placed around the sample holder and inserted into the bottom of the Teflon tube, which is already around the sample holder itself. This process allows the foam ring to expand inside the Teflon tube, thus restricting any air flow that could reach the sample. A second, larger foam ring is placed underneath the Teflon tube as a means of supporting it in the air, so that the Teflon tube can be moved up and down the length of the sample holder, allowing it to touch the bottom of the second temperature shielding component. An image of both the Teflon tube and foam rings is included below to provide visual context:

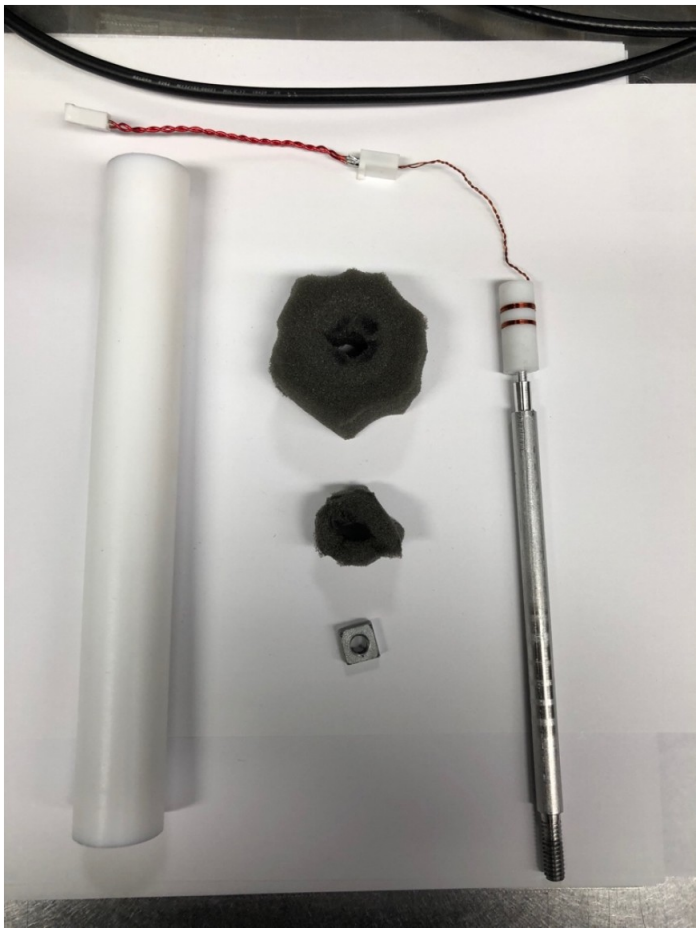

Fig. 14: (Shown left and center) Teflon tube and foam rings that make up key components of temperature shielding system

This second component of the temperature shielding system is an aluminum box that encapsulates the circuit board, restricting any effect that temperature fluctuations in the air may have on it. This aluminum box also has an aluminum lid which fastens to the rest of the enclosure through the use of four brass screws at each corner. This aluminum box, also known as the NMR probe box, measures 65.6 mm in width, 120.17 mm in length, and 39.85 mm in depth, easily fitting the circuit board which measures 62.86 mm in length and 52.20 mm in width. To accommodate for the various components of the NMR system that must attach to the circuit board, multiple holes had

to be made in the box and lid. The first hole in the box is on the bottom, to allow the wiring from the sample holder to attach to the two connectors on the bottom of the circuit board. The second hole made in the aluminum box was on the lid, so as to allow for the manipulation of the potentiometers while the system is in use. The third and fourth holes that were made in the aluminum box are for the BNC connectors that act as the input and output of the circuit board, allowing for the appropriate wires to attach the board to the rest of the NMR system. The final holes made in the box are two smaller holes in the bottom, whose purpose is to fasten the box to the new components to the new stability system put in place. A series of pictures is included below to allow better visualization of the box in question:

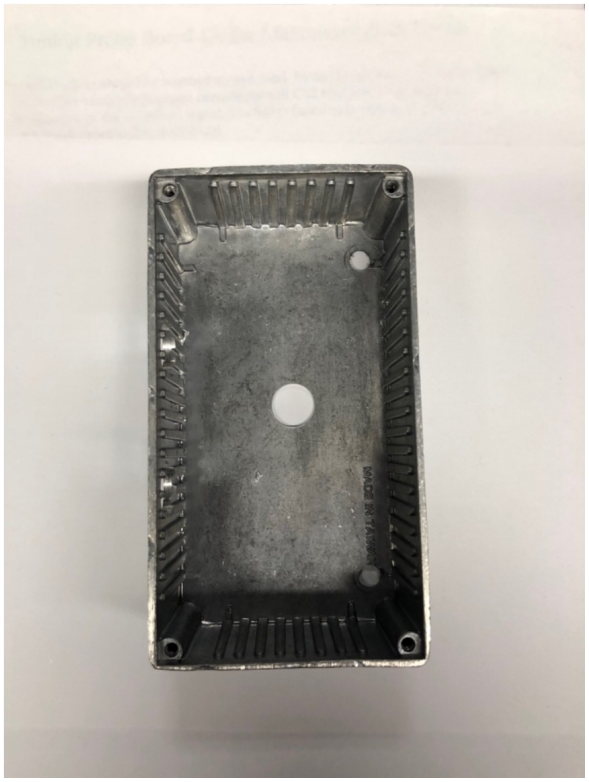

Fig. 15: Top-down view of aluminum box, showing center hole where wire around sample holder connects to circuit board

Fig. 16: Side-view of aluminum box, showing where BNC cables connect to Bridged-T circuit board

Fig. 17: Bottom side of aluminum box, two smaller holes indicating where hex screws go to secure box and circuit board to stability system

This new stability system, as previously mentioned, is designed to ensure the physical stability of the circuit board, so that there is no possible movement that could affect the results recorded through the NMR system. This system is rather simple, as it primarily consists of two parts, one vertical solid aluminum bar and one horizontal aluminum cross bar. The solid vertical bar attaches by one end to the magnet system through the use of two screws, thus guaranteeing that it acts as if it a part of the magnet's framework itself, as demonstrated in the image below:

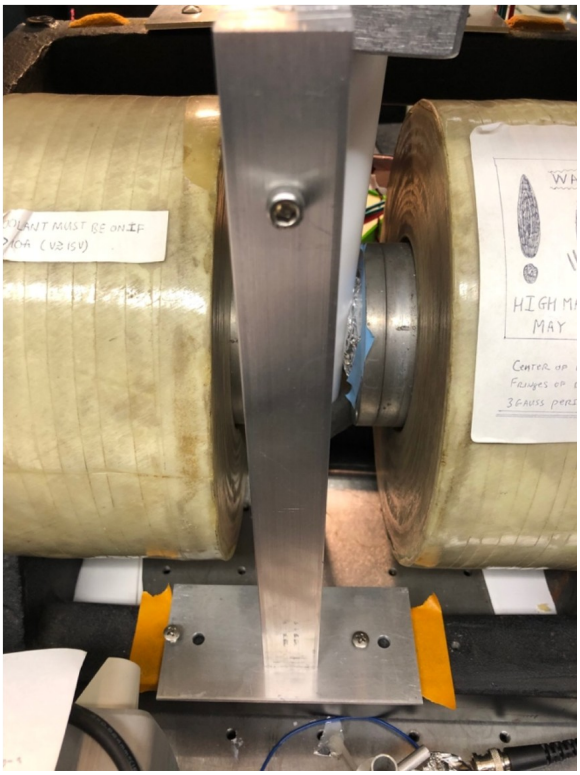

Fig. 18: Solid aluminum bar, one half of stability system

This solid bar then attaches to the horizontal cross bar through a screw that goes through a hole in the side of the vertical bar and twists into the hole found in the center of the cross bar. This cross bar is set above the magnet system and attaches to another part of the magnet's framework with another two screws, as seen in fig. 19:

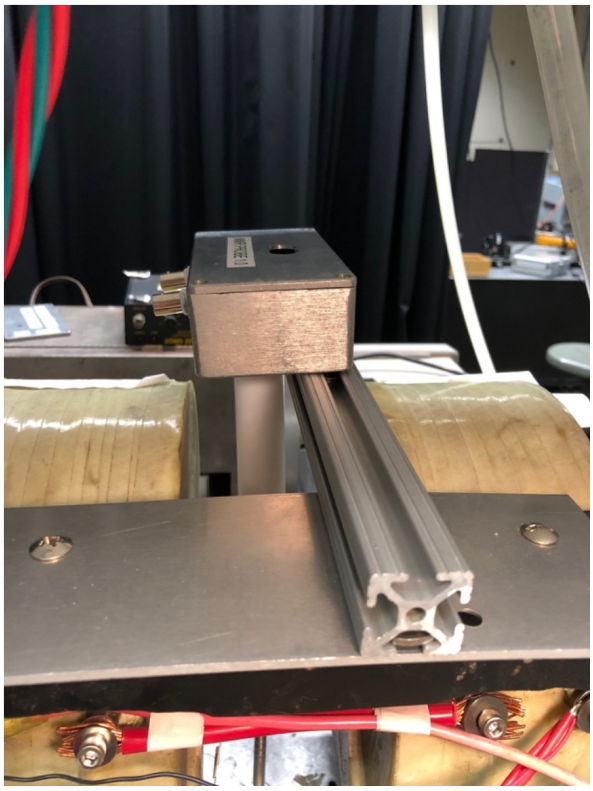

Fig. 19: Aluminum cross bar, one half of stability system

With both these bars in place and affixed solidly to the magnet's framework, one can then fasten the aluminum box to the side of the cross bar using the two additional holes in the bottom of the box, two hex screws, and two nuts that slip inside of top corrugated part of the cross bar, an image that can be at least partially demonstrated in the previous figure, as one may be able to observe the flat nut underneath the box. Altogether, this stability system securely fastens the circuit board to the magnet's framework, as well as positions the circuit board such that the sample holder and its own part of the temperature shielding structure are right below it.

Method:

With the intricacies of the NMR system properly explored in the preceding section, the next fundamental step in understanding this research project is to detail the method by which the relevant data was attained. The first part of this process to explain how one can attain the data found through this project begins by understanding how to ensure the NMR apparatus is properly started and functioning. Assuming all relevant equipment is properly connected in the manner previously described, the first step is to make certain that the magnet-cooling water supply is on, this water supply consisting of a series of tubes which runs water through the main magnet system. The next step is to make certain that the “auto voltage” switch, the smaller switch on the controller box, and the “field enable” switch, the larger switch on the controller box, are turned off (switch down), as shown in the picture below:

Fig. 20: Custom controller box, with “field enable” switch, “auto voltage” switch, “coarse field” knob, and “fine field” knob

Along with this, one must also make certain that the course field knob on the controller box is set to the correct starting point, so that the system is set at the correct starting voltage. Once these settings have been made, the next step involves turning on and setting-up the Fluke precision multimeter. This process, once performed, allows the multimeter to register the strength of the magnet, producing around 1V per Kilogauss and allowing the operator to know the strength of the magnet at any given time. Once the multimeter is properly set-up, the next pieces of the apparatus that must be addressed are the power supplies, the DC and the TCR. Once the DC then the TCR power supplies are started and set to the proper specifications for the experiment, the final part of the system that needs attention is the controller box. Through the controller box one enables both the field and the auto voltage, thus allowing the NMR system to function in the manner necessary for the experiments detailed in this project.

Once the startup sequence has been properly followed, the next step to attaining data from the NMR system requires turning on the remaining equipment within it, including the Lock-In Amplifier, the RF amplifier, both waveform generators, and the oscilloscope computer. Once each of these pieces of equipment are completely turned on and set to the correct settings, one can then begin running the Tekscope program on the oscilloscope's desktop. This Tekscope program is what allows the oscilloscope computer to act as an oscilloscope and, if the setup and startup sequence were followed correctly, two lines, in this case yellow and blue indicating the in-phase and quadrature components of the signal, should appear within the Tekscope display. The next step is to balance the Bridged-T circuit. Having these two lines appear may require some more fine adjustments, including but not limited to, changing the setting on the signal

sensitivity knob on the Lock-In Amplifier, adjusting the frequency on waveform generator #1 which provides the initial frequency that acts as the input for the circuit board, and adjusting the two potentiometers on top of said circuit board. These lines represent the in-phase and in-quadrature components of the signal, and the next step of the process involves zeroing them. The method one employs to zero them involves adjusting the RF frequency to bring the in-quadrature components close to zero and adjusting the potentiometers on top of the circuit board to bring the in-phase component to zero. Once these adjustments are made, one then turns the signal sensitivity knob on the Lock-In Amplifier counter-clockwise to the next lowest voltage setting. This process of adjustment and lowering the signal sensitivity setting is repeated until both the in-phase and in-quadrature components are both close to zero while the signal sensitivity knob is set to 1 mV. Once both lines appear at the 1 mV setting, adjustments are made to decrease the difference between them to around the length of 2 distance units as presented on the margins of the oscilloscope display. From here one can then begin increasing the magnetic field to the initial estimation of where the resonance will most likely appear, based on the frequency set on the first waveform generator divided by the gyromagnetic ratio for a proton, 42.5774806 MHz/T.

Following this increase in the magnetic field, one then goes into the settings of the Tekscope program and switches it from DC to AC, so as to limit any slow voltage wandering that may occur while in the process of finding the resonance. Once the magnetic field has been increased to the estimated strength, indicated through the voltage on the multimeter, then one can begin magnetic-field sweeping through the control voltage using the course and field knobs. This sweep continues until a visual

bump in the lines is observed, indicating at what voltage and field strength the resonance occurs at. Once this range is narrowed down, one then changes more of the oscilloscope's settings, so as to allow said bump in the signal to be more easily observed. This process also involves turning on the dither created through the second waveform generator, establishing an automatic sweep in the voltage on the multimeter, that also appear on the screen of the oscilloscope through channel 3. This dither allows the one performing the experiment to observe this bump repeatedly without having to manually operate the controller box. The final step in cleaning up the resonance involves changing another setting on the oscilloscope, altering the sampling method from instant to the average over 50 points. This change in the sampling method means that each observation of the resonance peak that occurs per second is averaged to give a clear picture that eliminates some of the inherent noise of the signal. This process of cleaning up the signal will also involve making slight adjustments to the multimeter voltage so that the resonance peak appears around the middle of the dither.

Once this mixed resonance peak is established, one then begins recording all relevant data by creating csv files for all three channels, as well as saving the set-up in a different type of file. The process continues by then physically recording the frequency and voltage at which it occurred and the voltage and time of the dither sweep. The process by which one finds the absorptive and dispersive components of the resonance peak is by altering the frequency output by the first waveform generator, increasing the frequency to find the dispersive component and decreasing the frequency to find the absorptive component. Once all of this relevant information is properly recorded, said files can then be transferred to the main laboratory computer for further processing and

calculation. For future reference, one should note that most if not all results included in the results section are derived from the dispersive component of each resonance peak, as said component was the most clearly observed and the most functional for the following calculations necessary to accurately measure the height and width of the peak.

The final step of the process to attain the data in a relevant format involves performing the calculations necessary to create the graphs to demonstrate the interaction between the height and width of the resonance peak and the concentration of the potassium permanganate. These calculations are best summarized as factoring in the ratio of volts per second as measured on the oscilloscope through the dither and multiplying it by the ratio of gauss per volt set through the magnet system. The resulting product is the gauss per second for the data sample, which is then applied through multiplication to the measured time in the csv file, which through the open source data analysis program SciDAVis, takes the form of a column on a datasheet. Once applied to the measured time and creating a new column which demonstrates the change in gauss from the magnet, this column is then compared to the channel 1 resonance in arbitrary units and the channel 3 dither also in arbitrary units. Once these data columns are properly set, one can then create a graph using the three columns, with the gauss of the magnetic field acting as the x-axis and the arbitrary unit columns functioning as the y-axis. The rest of the process involves reformatting the resulting graph to fit the standardized axes ranges of -0.01 to 0.01 for channel 1 resonance, -3 to 3 for channel 3 dither, and a range of 6 gauss for the magnetic field, it not having a set gauss range as it can vary from sample to sample. This finalization process also involves applying a

moving window average of 100 to the channel 1 resonance, to reduce the noise present and give a clearer image of the dispersive resonance component. Once this moving window average is appended to the graph, one can then measure the resonance peak's width by measuring the distance in gauss between the negative peak and positive peak inherent to the dispersive component and measuring the height through the height of the positive peak, both of which are done precisely through another data table provided by the SciDAVis program.

It should be noted for the sake of documenting the history of the research project, there were many changes and alterations to the method that occurred over the course of the research period. The first primary change in the method was that, initially, the signal knob setting of the Lock-In Amplifier was set to 100 microvolts, rather than 1 mV as in the final process. This alteration to the signal sensitivity setting occurred because, while exploring the capabilities of the system, it was discovered that the resonance peak could still be observed at the higher signal setting, as well as present a great opportunity to change the sampling from real-time to average over a period of time, leading to a much clearer image. With both these facts in mind, it made sense to change the setting for all future tests as it would allow for the resonance peak to be measured more easily.

One should also note that, in the initial tests that were performed for this research project, only the mixed signal was recorded and analyzed, as it was not yet discovered that the resonance peak could be separated into its absorptive and dispersive components. Knowing this, it should be no surprise then that the results produced by this earlier method are less than optimal in displaying the behavior the tests are intended

to demonstrate. Once it was realized that the absorptive and dispersive components of the resonance peak could be observed separately, the only change necessary to the process was to, after recording the relevant data for the mixed resonance peak, go about finding the separated components and recording them in the same manner.

Data/Results:

Before presenting and analyzing the data recorded through the finalized data collection process, it seems imperative for understanding the history of the research project that one also observes the data collected through the initial method. One example is easily observed below in the following figure:

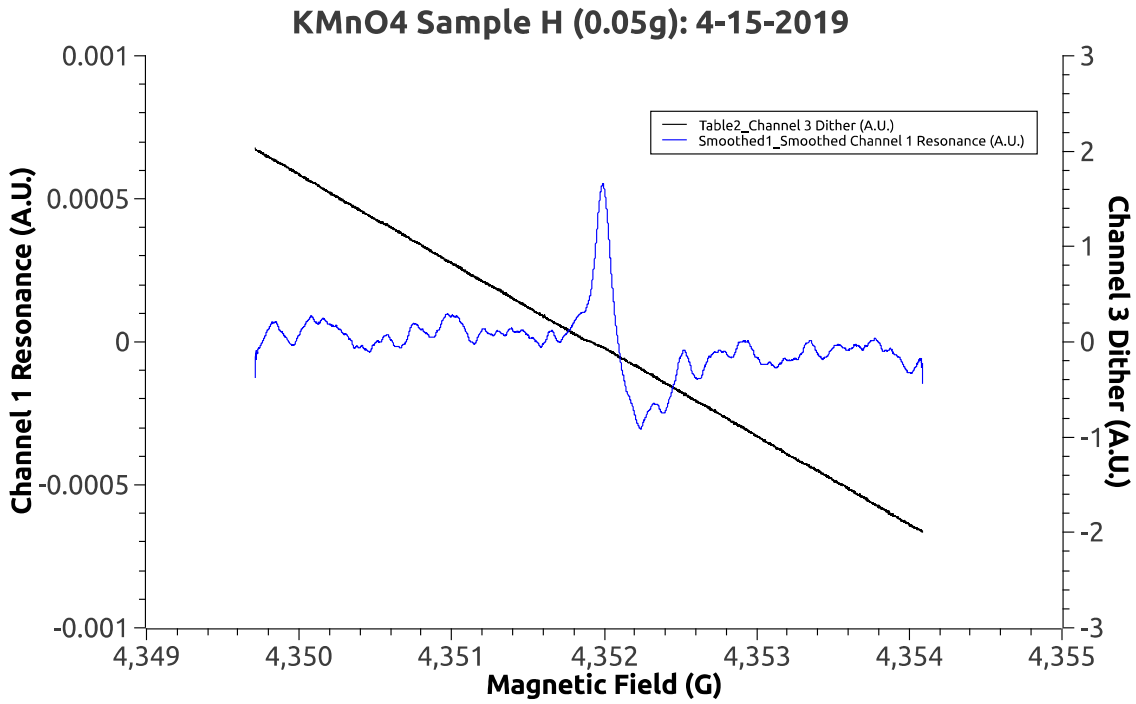

Fig. 21: Mixed resonance graph for $KMnO_4$ Sample H

This graph, while providing a representation of the resonance, does so by presenting the mixed resonance peak of the sample. One can tell that the resonance demonstrated through the graph is a mixed resonance peak due to the fact that, unlike a purely dispersive component, demonstrates a difference in the positive peak and the negative peak. While a purely dispersive signal would be antisymmetric, this resonance shows the negative peak having a smaller amplitude that increases to zero at a much slower rate than the positive peak. It is due to this difference in the positive and negative peaks

that attempting to measure the height and width of the resonance is harder than simply measuring the dispersive component, as the means by which one measures the absorptive and dispersive components of the resonance, each of which is a part of the mixed resonance signal, differs greatly. So, when one attempts to measure the height and width of a mixed signal, it is not abundantly clear which method of measurement is applicable, be the absorptive, dispersive, or some calculated mix of the two.

With the finalized method successfully followed and the necessary calculations completed, one can now analyze and discuss the results derived by the experiments performed for this research project. Before examining the overall results derived, it feels vital that this project present some examples of the individuals results, so as to further demonstrate how the trends were analyzed. Included below are some examples of the dispersive resonance components observed using the data recorded through the oscilloscope and the graphing program known as SciDAVis:

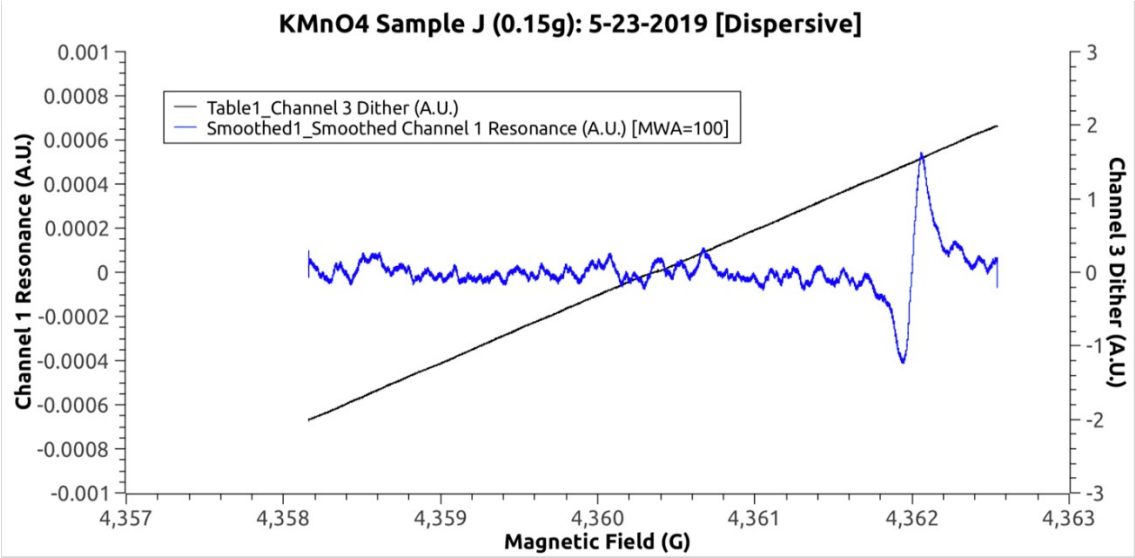

Fig. 22: Dispersive resonance graph for $KMnO_4$ Sample J

From these graphs alone, one can garner some indication that these results lend themselves to a more straightforward analysis than previous data collection efforts. This increased sense of trust comes from the fact that said graphs predominantly resemble typical dispersive components of the resonance. This is significant as, with this certainty that the resonance observed in the above graphs are primarily the dispersive component, that means the method of measuring the width, that being measuring the distance between the positive and negative peak, is all the more likely to be accurate.

With this new understanding of the individual results established, one is now able to better understand how these results function when examined together. Included below is the complete set of all finalized data for the thesis project. This data includes both the individual graphs for all recorded samples as well as tables which demonstrate, in terms of arbitrary units for height and Gauss for width, the change that occurs in the resonance peak through the alteration of the concentration of the potassium permanganate dissolved in the H_2O solution:

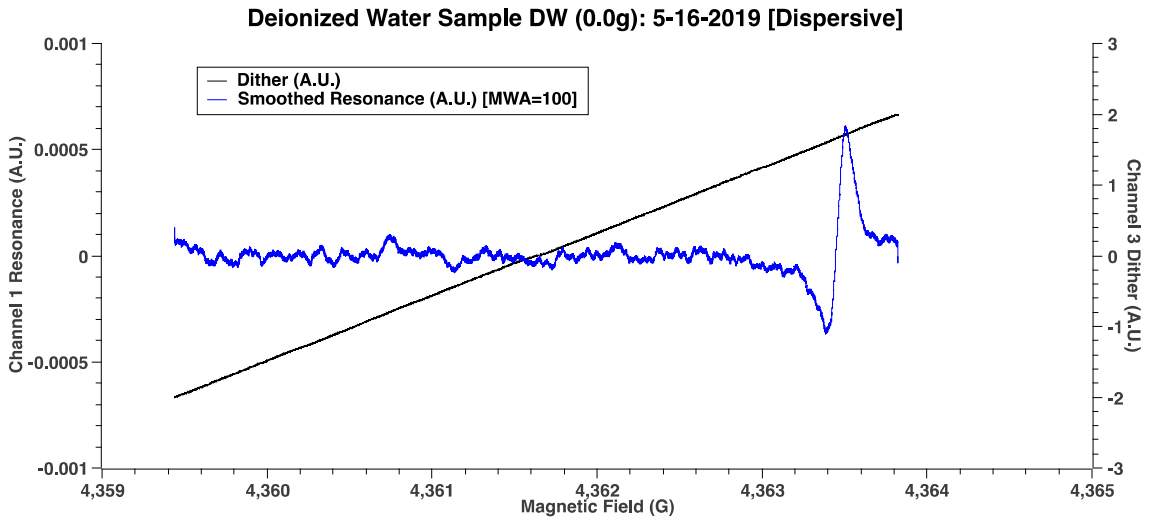

Fig. 23: Dispersive resonance graph for Deionized Water sample DW (5-16-2019)

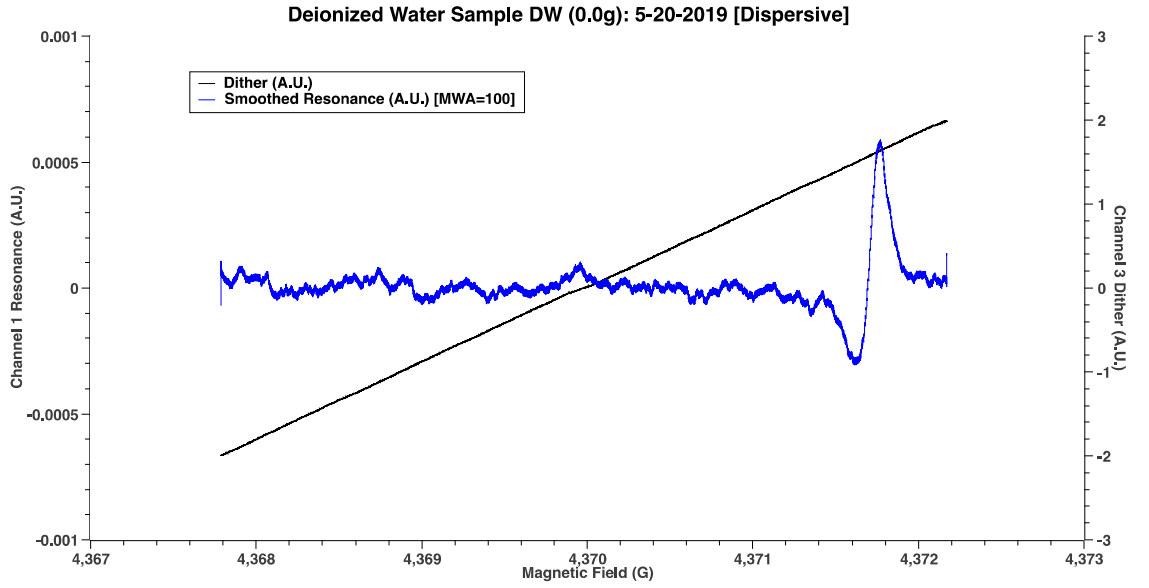

Fig. 24: Dispersive resonance graph for Deionized Water sample DW (5-20-2019)

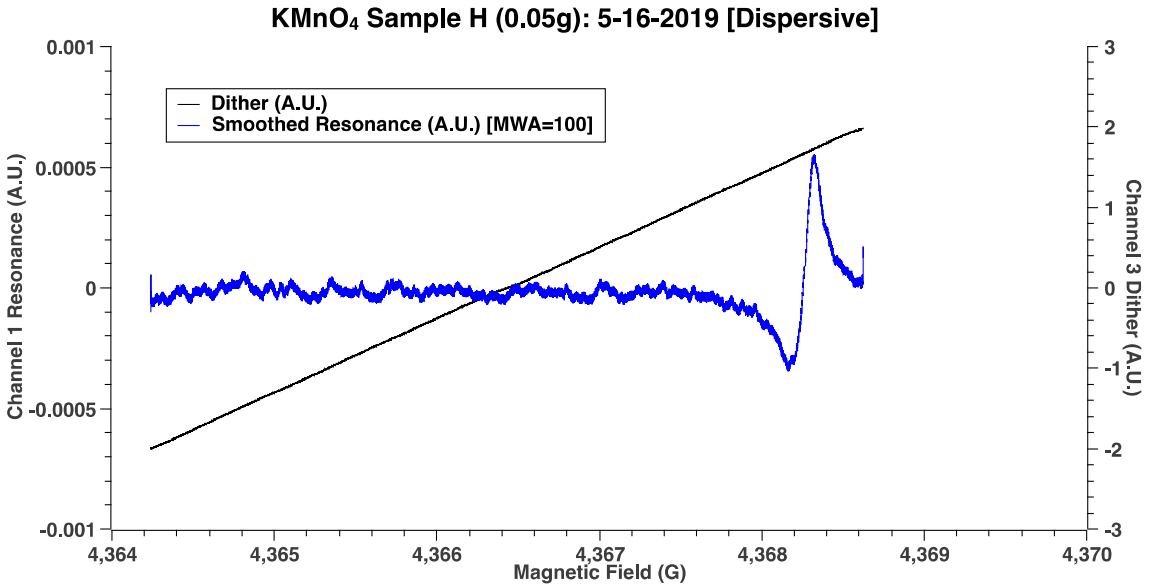

Fig. 25: Dispersive resonance graph for $KMnO_4$ Sample H (5-16-2019)

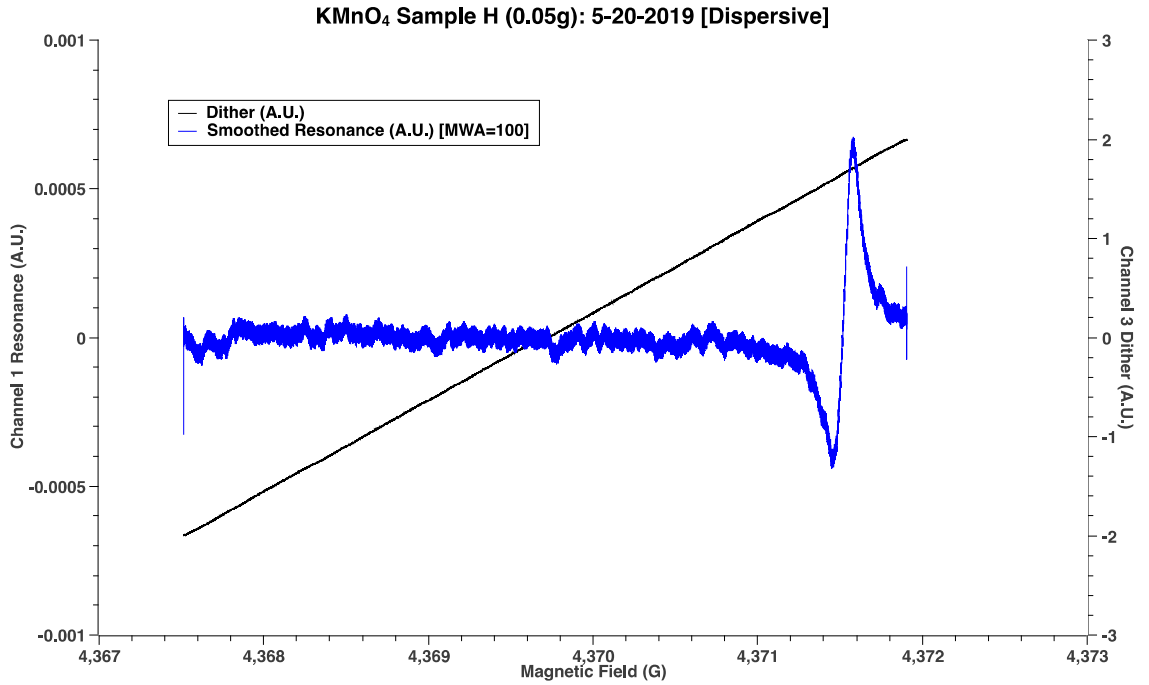

Fig. 26: Dispersive resonance graph for $KMnO_4$ Sample H (5-20-2019)

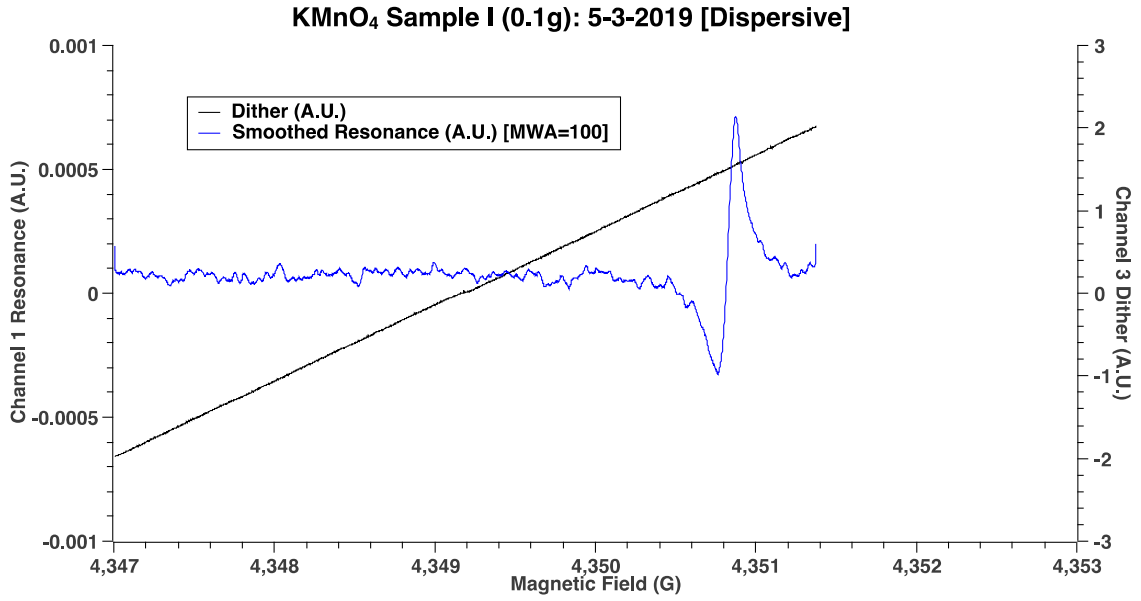

Fig. 27: Dispersive resonance graph for $KMnO_4$ Sample I (5-3-2019)

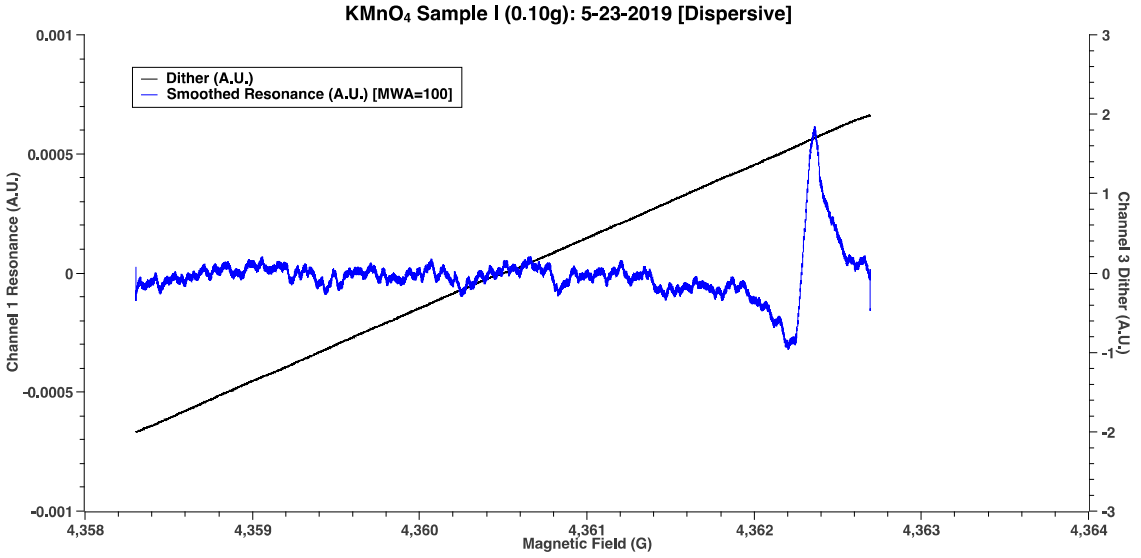

Fig. 28: Dispersive resonance graph for $KMnO_4$ Sample I (5-23-2019)

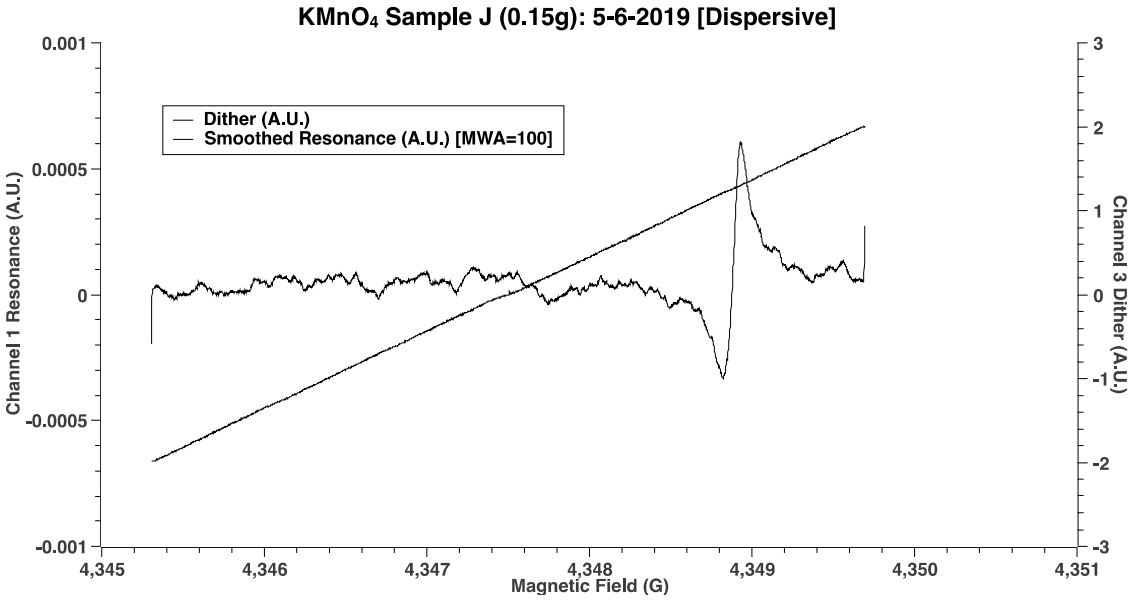

Fig. 29: Dispersive resonance graph for $KMnO_4$ Sample J (5-6-2019)

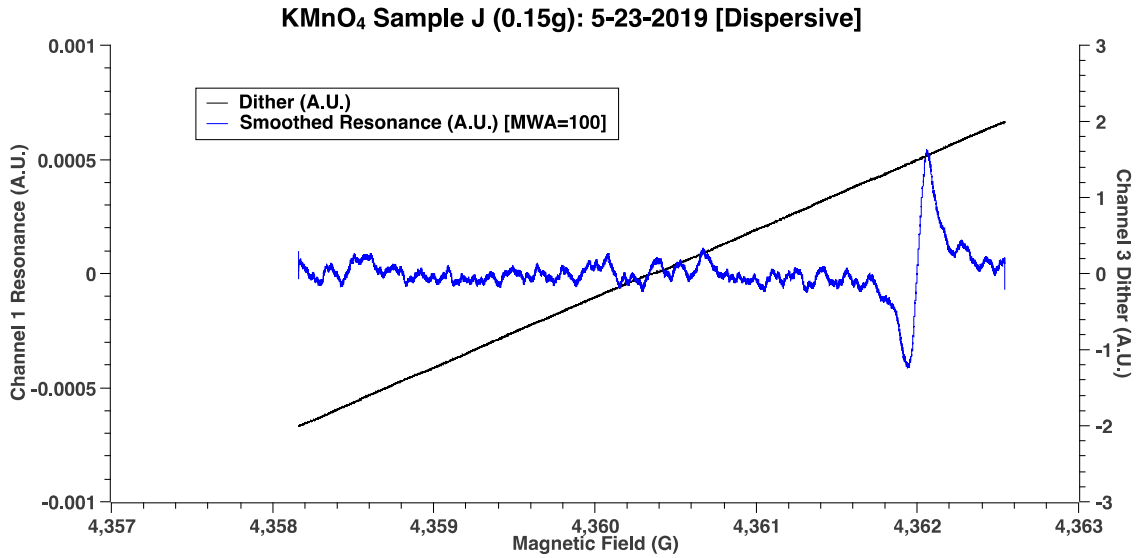

Fig. 30: Dispersive resonance graph for $KMnO_4$ Sample J (5-23-2019)

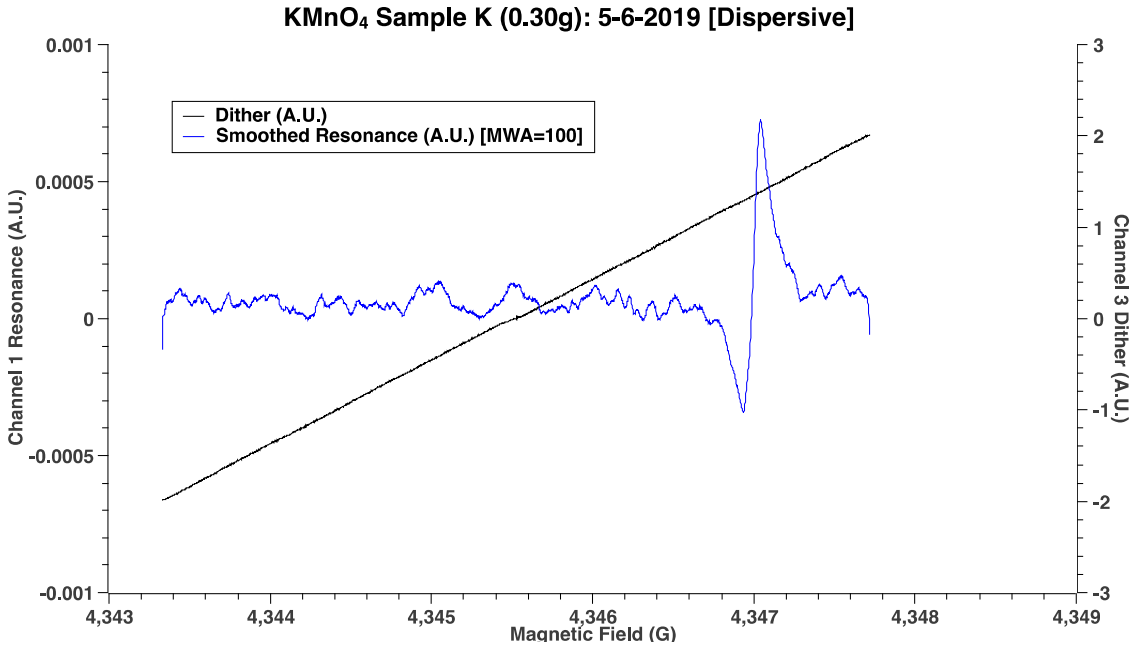

Fig. 31: Dispersive resonance graph for $KMnO_4$ Sample K (5-6-2019)

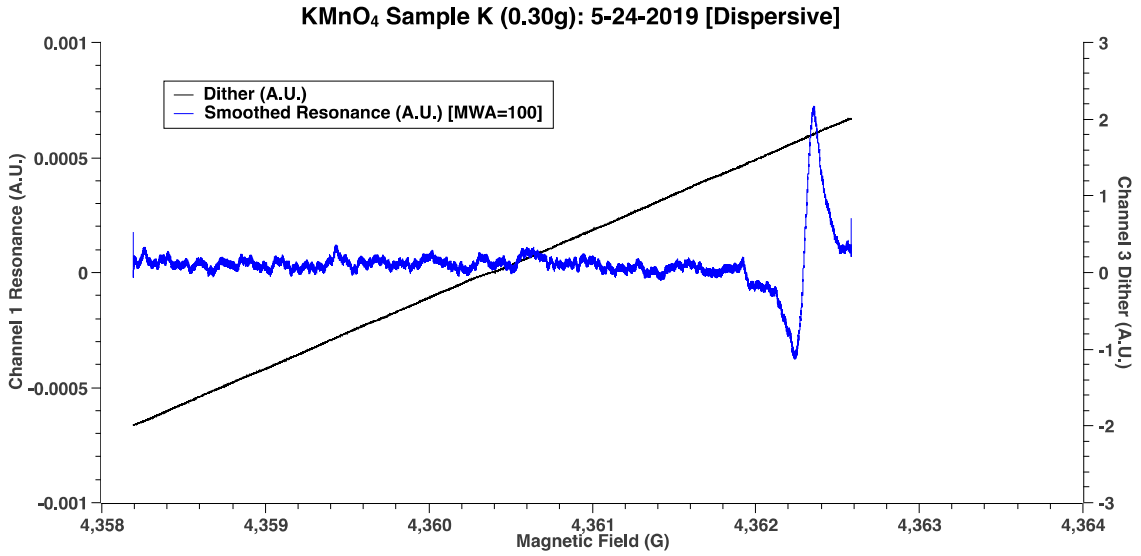

Fig. 32: Dispersive resonance graph for $KMnO_4$ Sample K (5-24-2019)

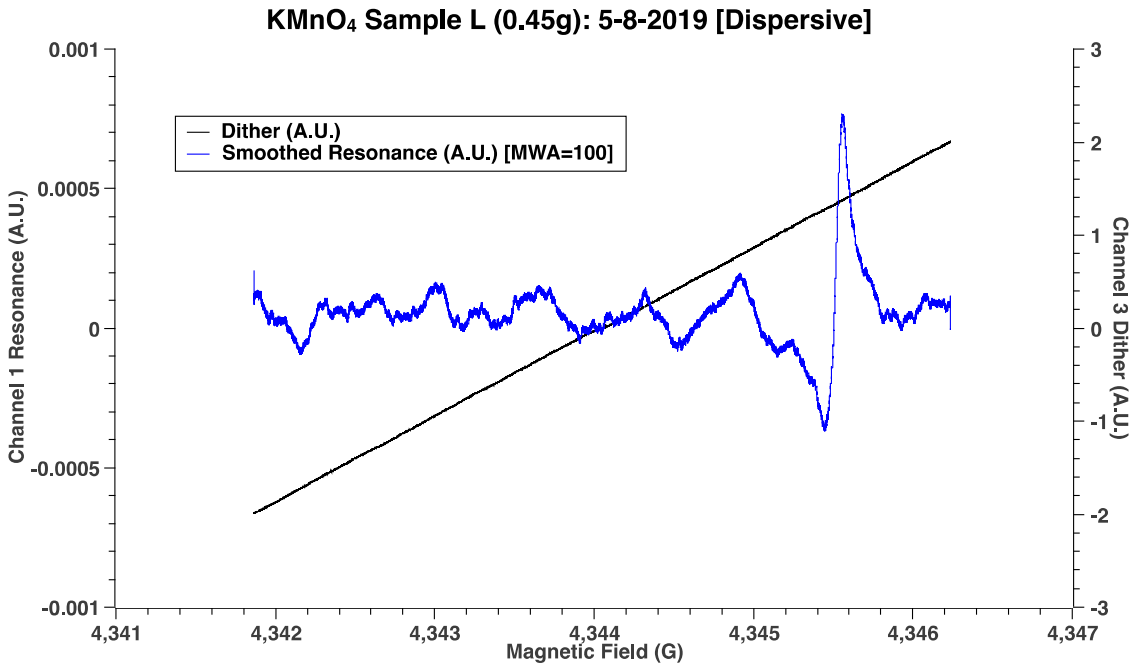

Fig. 33: Dispersive resonance graph for $KMnO_4$ Sample L (5-6-2019)

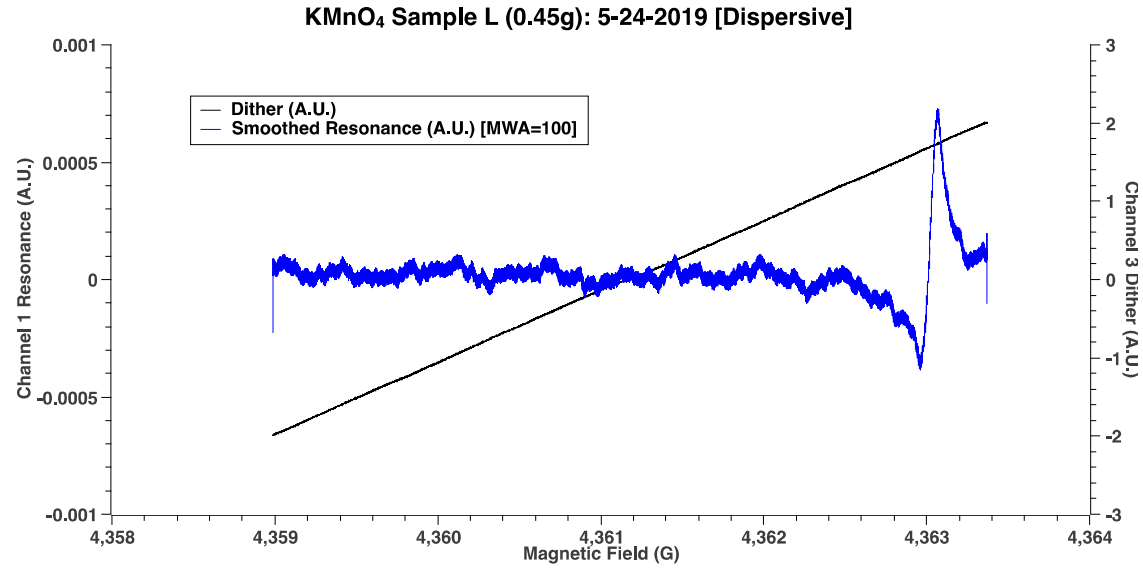

Fig. 34: Dispersive resonance graph for $KMnO_4$ Sample L (5-24-2019)

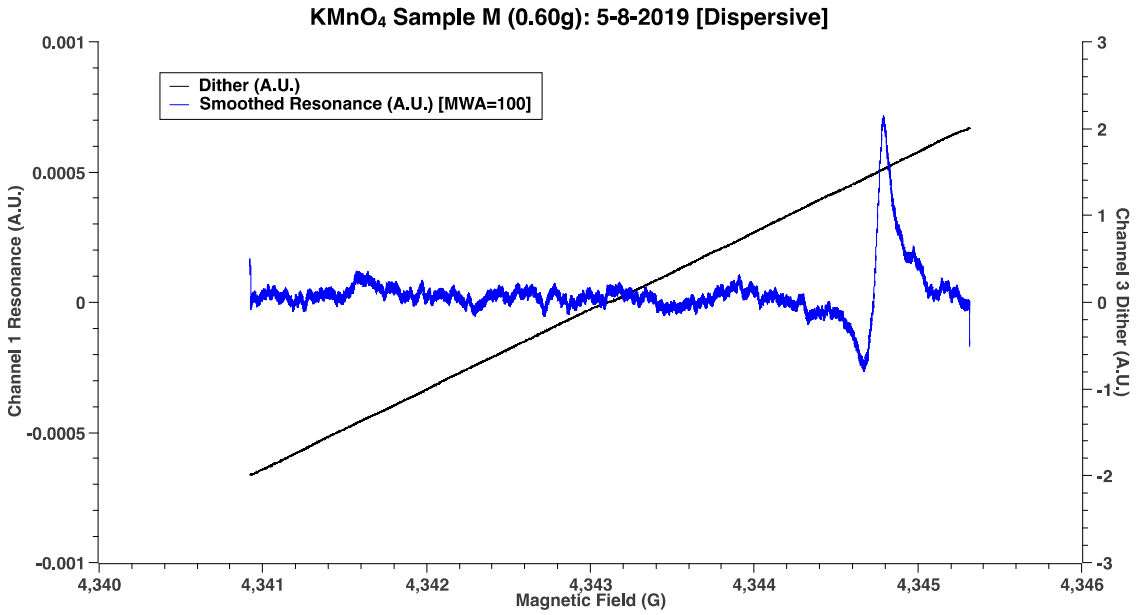

Fig. 35: Dispersive resonance graph for $KMnO_4$ Sample M (5-8-2019)

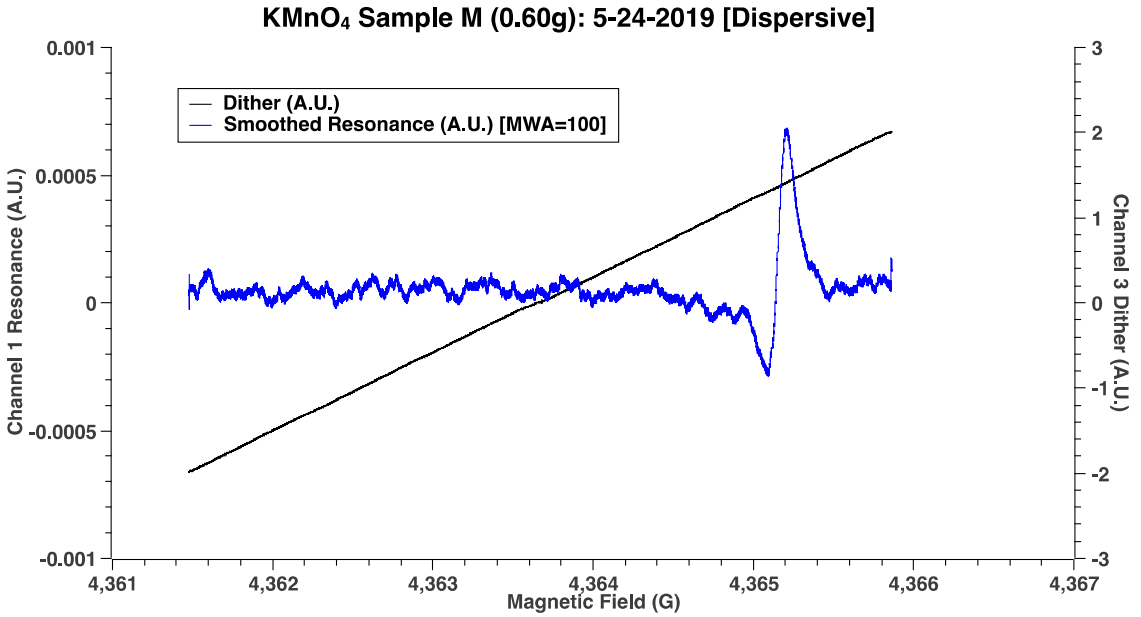

Fig. 36: Dispersive resonance graph for $KMnO_4$ Sample M (5-24-2019)

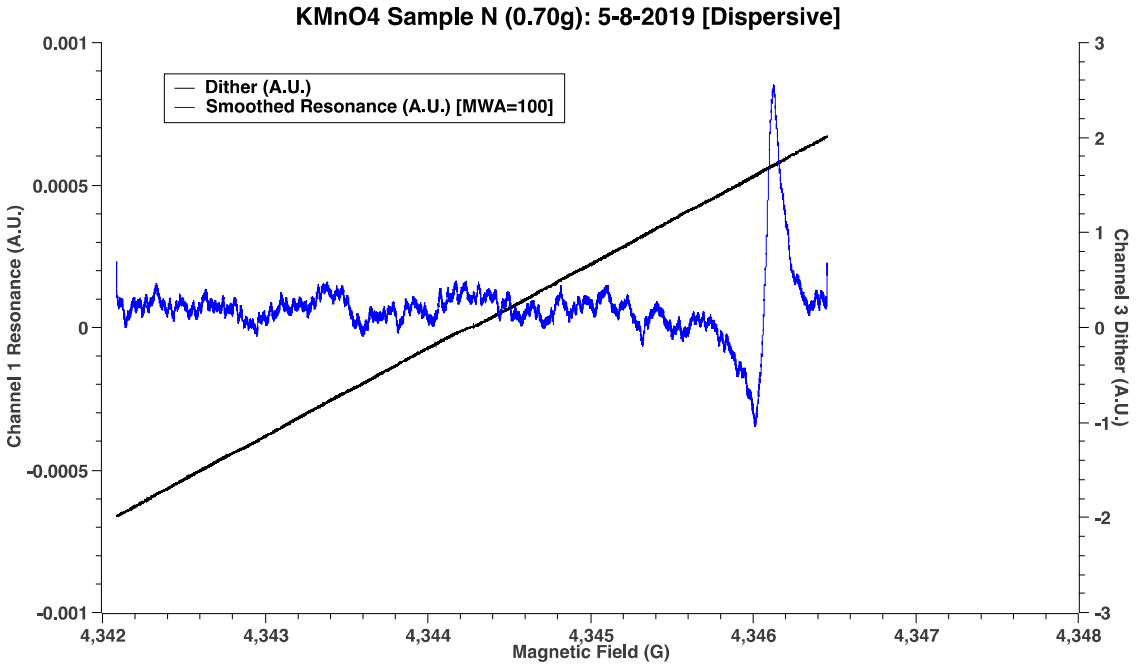

Fig. 37: Dispersive resonance graph for $KMnO_4$ Sample N (5-8-2019)

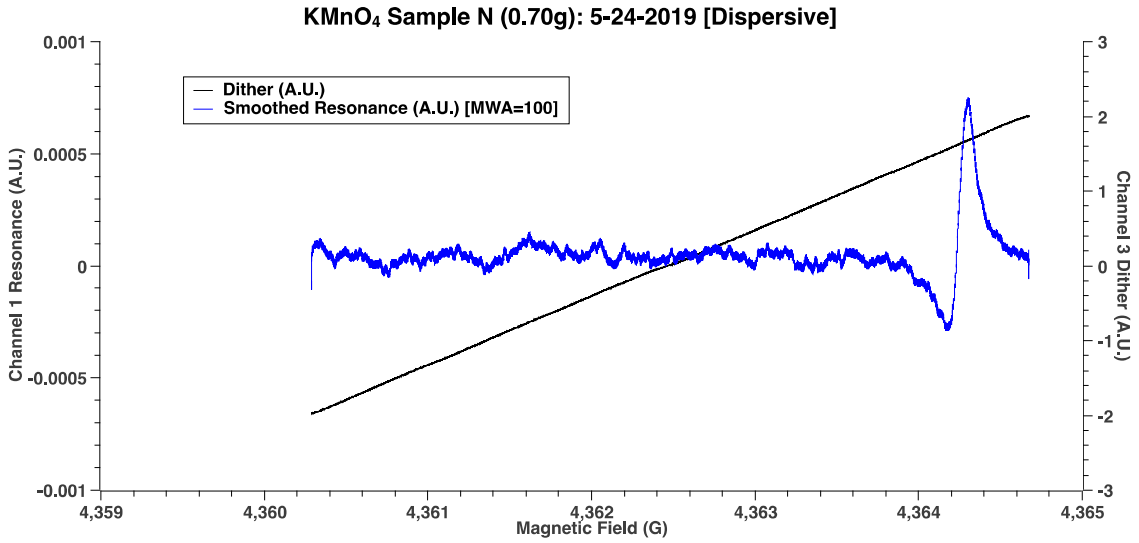

Fig. 38: Dispersive resonance graph for $KMnO_4$ Sample N (5-24-2019)

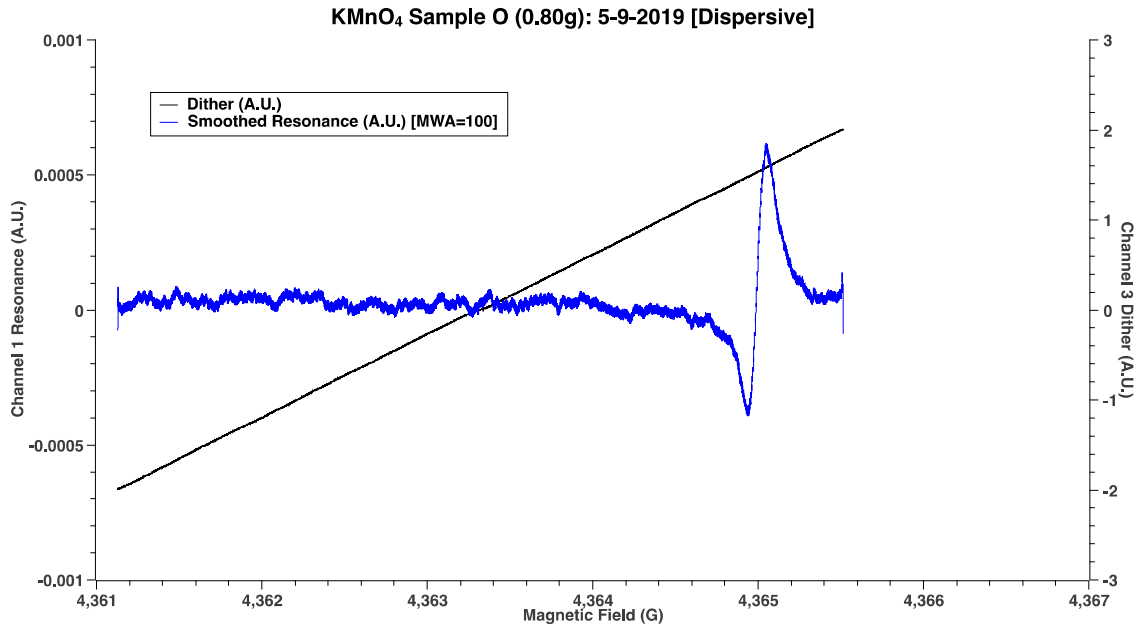

Fig. 39: Dispersive resonance graph for $KMnO_4$ Sample O (5-9-2019)

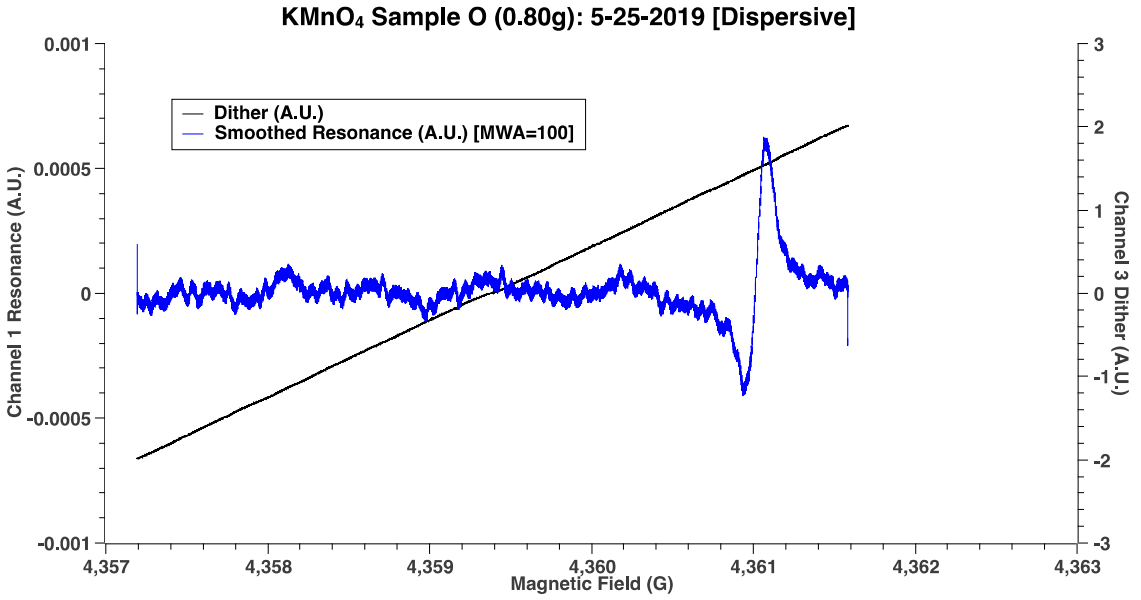

Fig. 40: Dispersive resonance graph for $KMnO_4$ Sample O (5-25-2019)

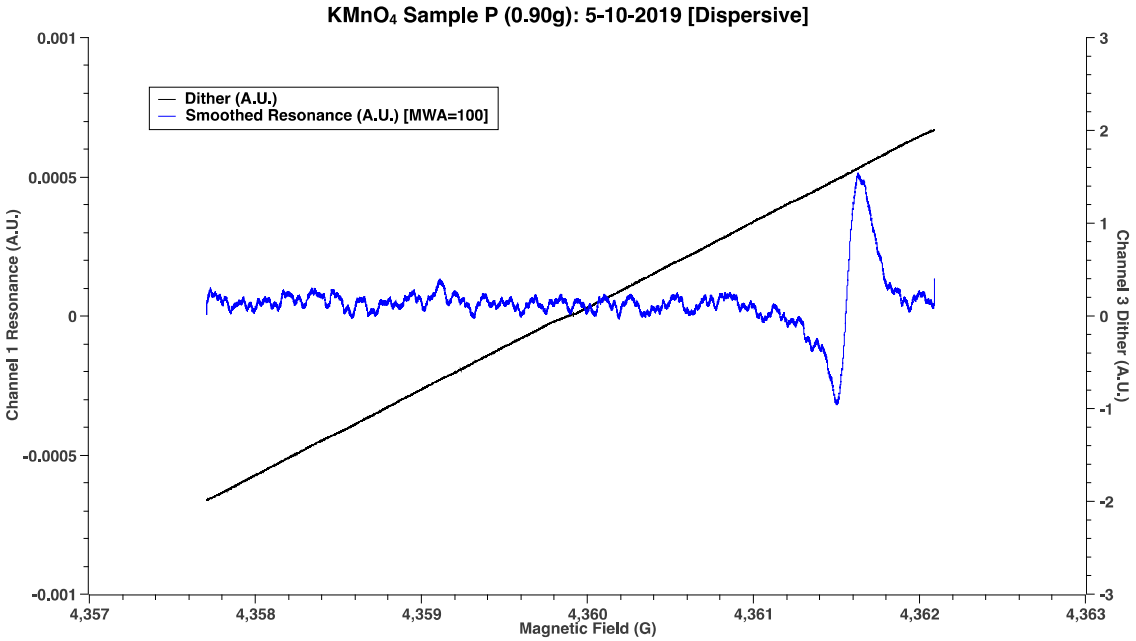

Fig. 41: Dispersive resonance graph for $KMnO_4$ Sample P (5-10-2019)

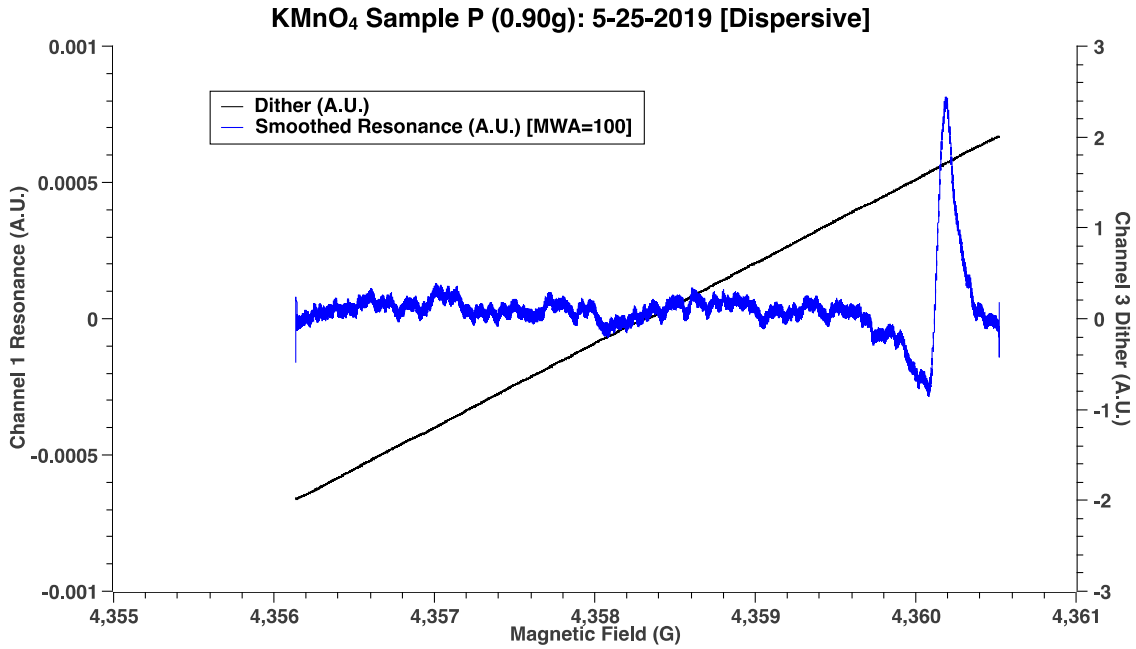

Fig. 42: Dispersive resonance graph for $KMnO_4$ Sample P (5-25-2019)

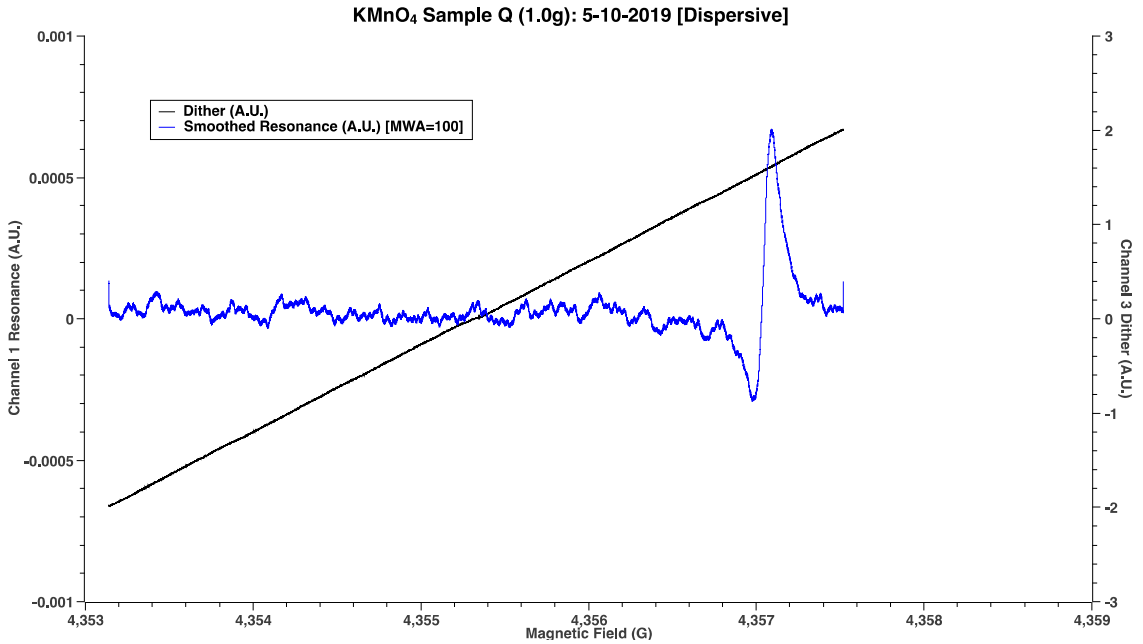

Fig. 43: Dispersive resonance graph for $KMnO_4$ Sample Q (5-10-2019)

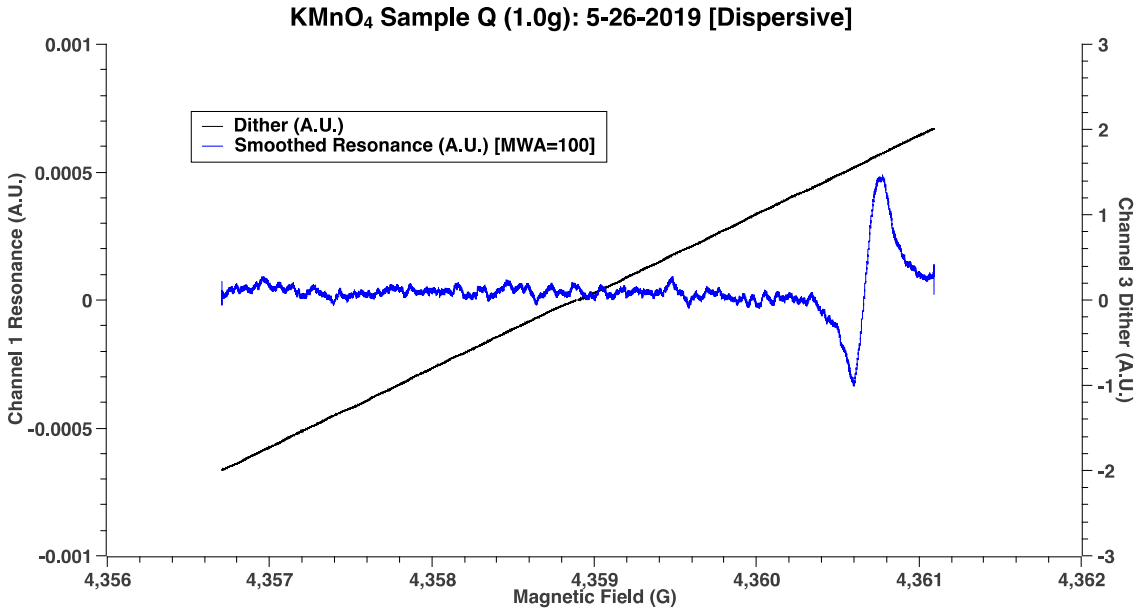

Fig. 44: Dispersive resonance graph for $KMnO_4$ Sample Q (5-26-2019)

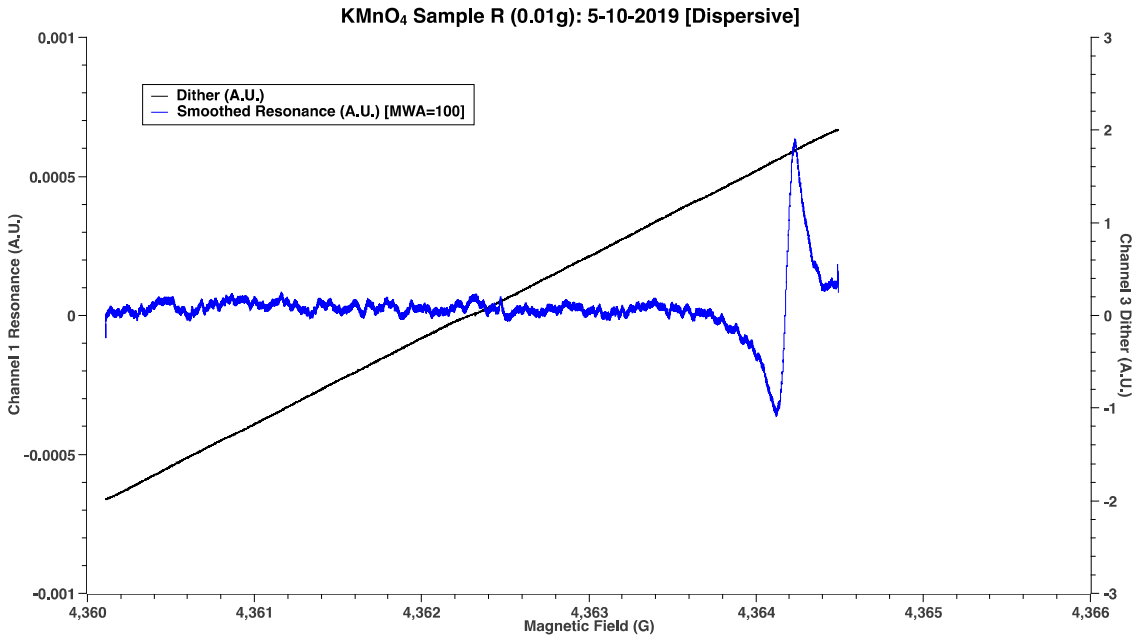

Fig. 45: Dispersive resonance graph for $KMnO_4$ Sample R (5-10-2019)

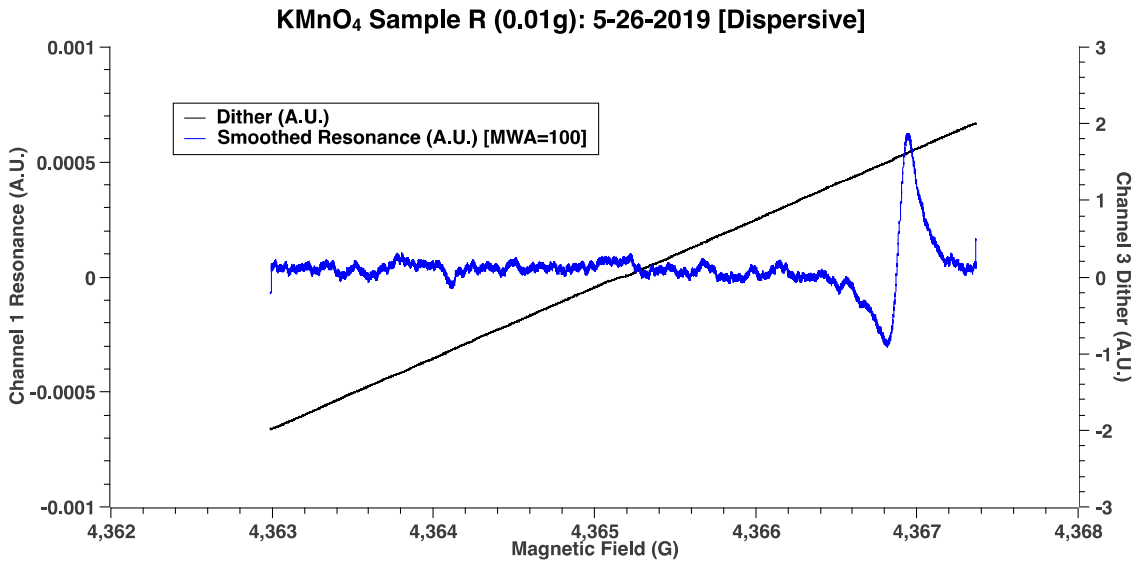

Fig. 46: Dispersive resonance graph for $KMnO_4$ Sample R (5-26-2019)

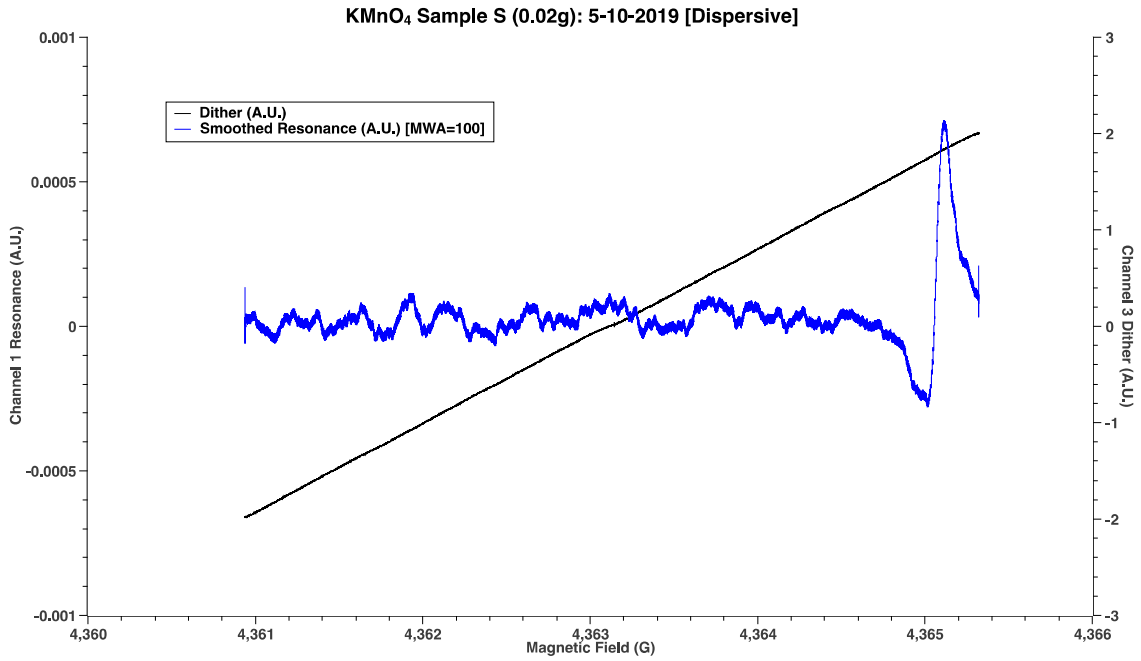

Fig. 47: Dispersive resonance graph for $KMnO_4$ Sample S (5-10-2019)

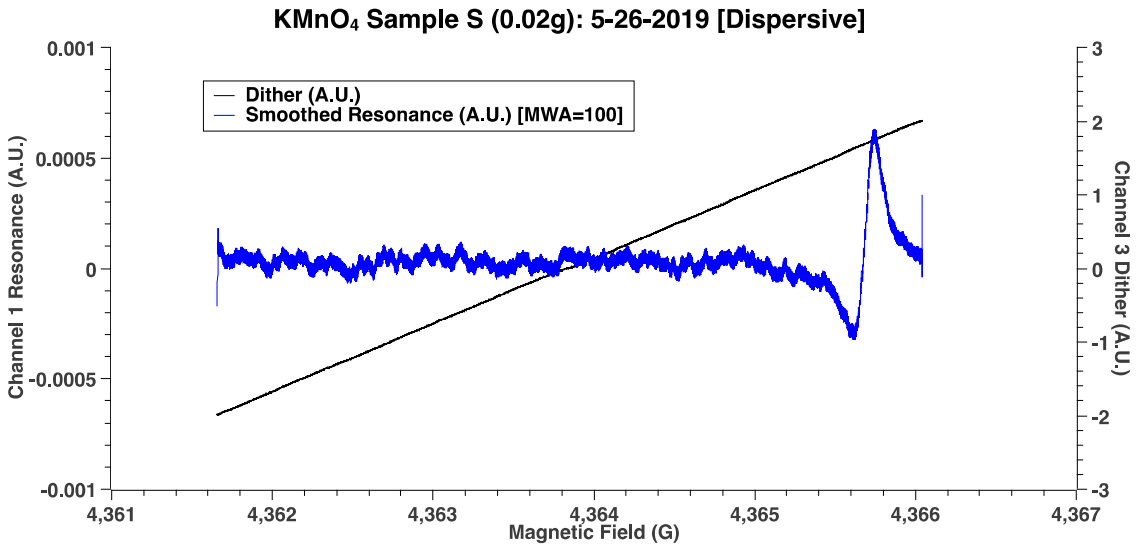

Fig. 48: Dispersive resonance graph for $KMnO_4$ Sample S (5-26-2019)

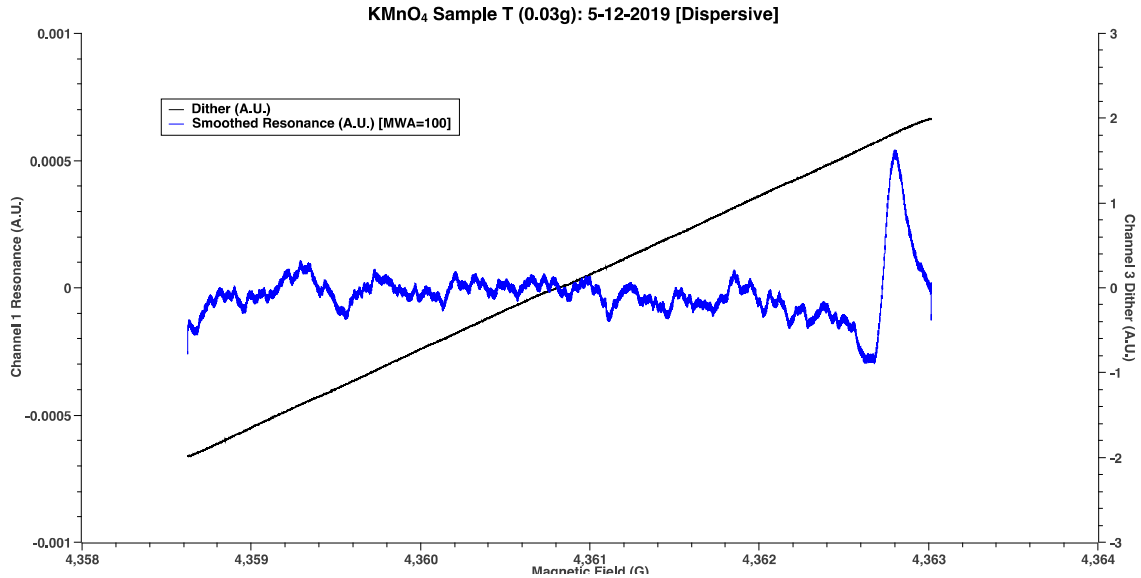

Fig. 49: Dispersive resonance graph for $KMnO_4$ Sample T (5-12-2019)

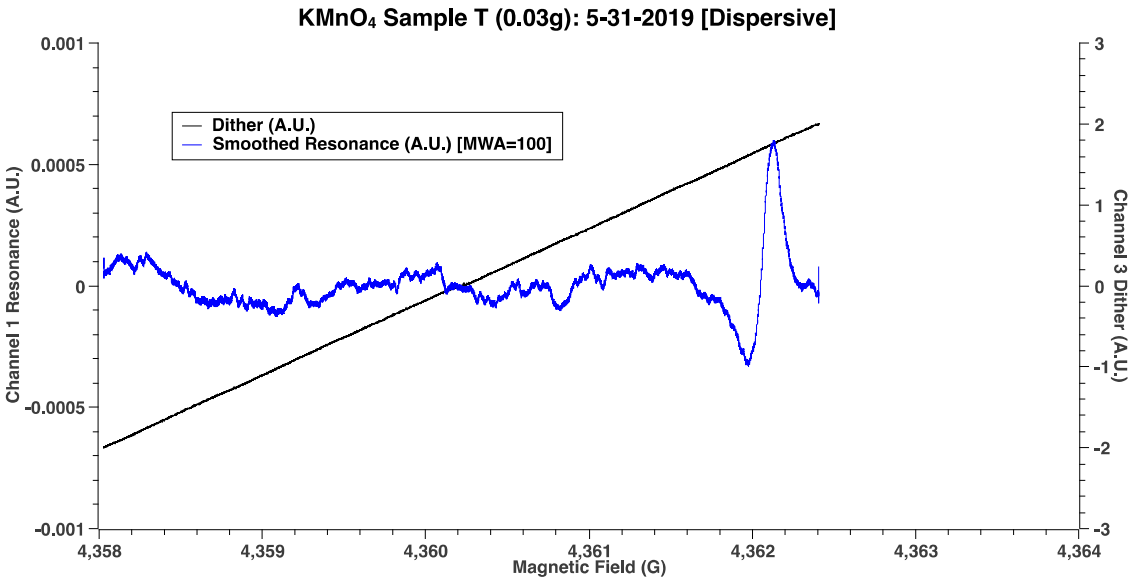

Fig. 50: Dispersive resonance graph for $KMnO_4$ Sample T (5-31-2019)

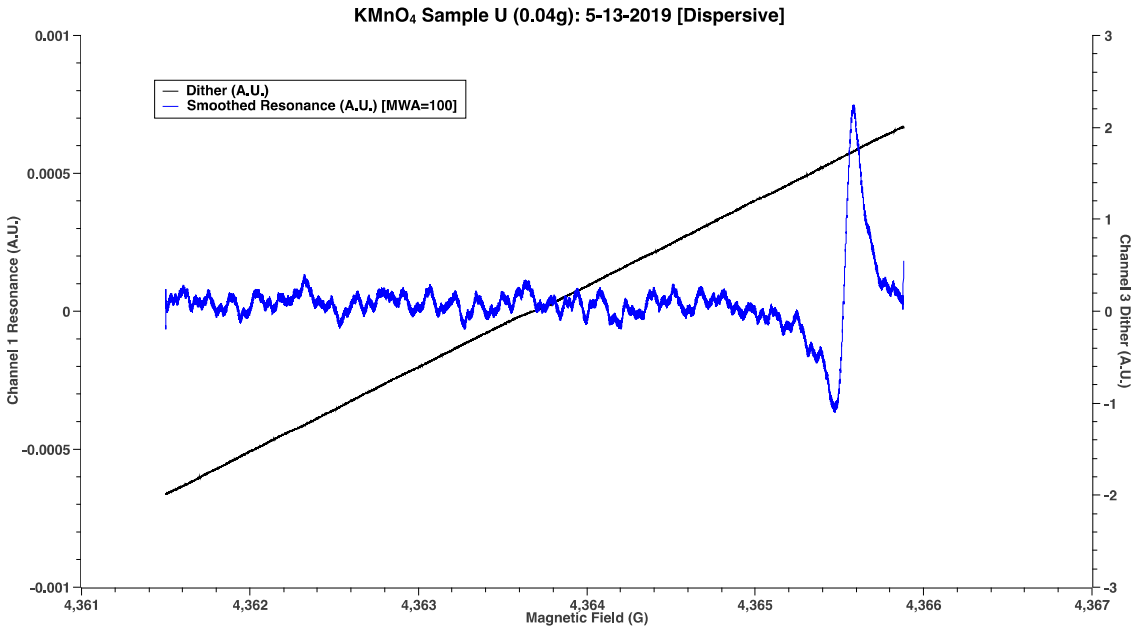

Fig. 51: Dispersive resonance graph for $KMnO_4$ Sample U (5-13-2019)

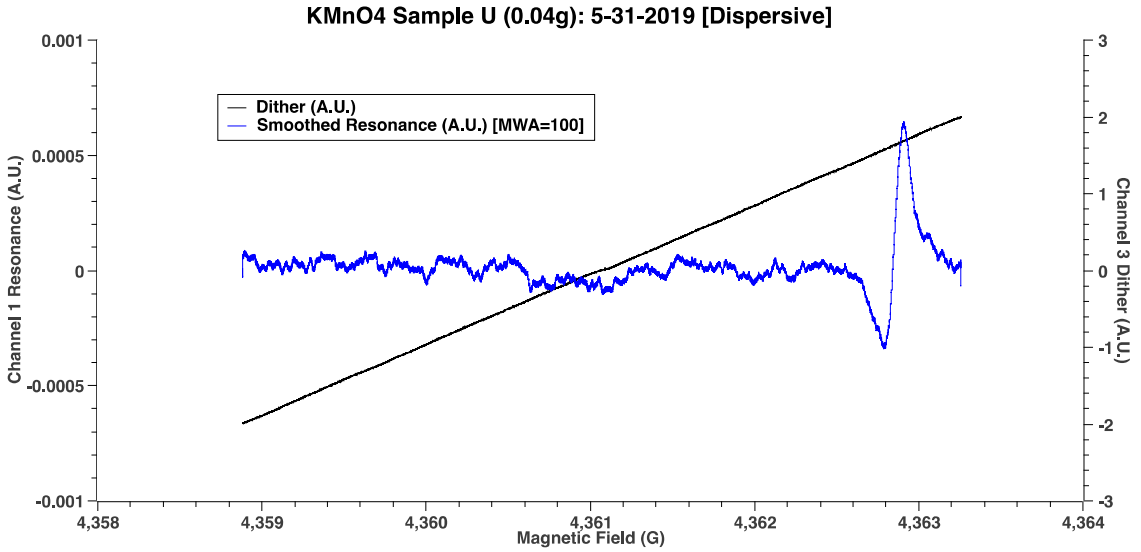

Fig. 52: Dispersive resonance graph for $KMnO_4$ Sample U (5-31-2019)

Figs. 23-52 are supposed to demonstrate how the varying of concentration of $KMnO_4$ can affect the height and width of the observed dispersive resonance peak.

Sample	Concentration	Run 1	Run 2	Average
Deionized Water DW	0g/100ml	Height = 0.00061 A.U. Width = 0.118 gauss	Height = 0.00059 A.U. Width = 0.145 gauss	Height = 0.00060 A.U. Width = 0.136 gauss
R	0.01g/100ml	Height = 0.00063 A.U. Width = 0.114 gauss	Height = 0.00063 A.U. Width = 0.126 gauss	Height = 0.00063 A.U. Width = 0.120 gauss
S	0.02g/100ml	Height = 0.00071 A.U. Width = 0.107 gauss	Height = 0.00063 A.U. Width = 0.126 gauss	Height = 0.00067 A.U. Width = 0.116 gauss
T	0.03g/100ml	Height = 0.00054 A.U. Width = 0.118 gauss	Height = 0.00060 A.U. Width = 0.157 gauss	Height = 0.00057 A.U. Width = 0.137 gauss
U	0.04g/100ml	Height = 0.00075 A.U. Width = 0.111 gauss	Height = 0.00065 A.U. Width = 0.126 gauss	Height = 0.00070 A.U. Width = 0.118 gauss
H	0.05g/100ml	Height = 0.00055 A.U. Width = 0.164 gauss	Height = 0.00067 A.U. Width = 0.130 gauss	Height = 0.00061 A.U. Width = 0.147 gauss
I	0.10g/100ml	Height = 0.00071 A.U. Width = 0.111 gauss	Height = 0.00061 A.U. Width = 0.153 gauss	Height = 0.00066 A.U. Width = 0.131 gauss
J	0.15g/100ml	Height = 0.00061 A.U. Width = 0.109 gauss	Height = 0.00055 A.U. Width = 0.114 gauss	Height = 0.00058 A.U. Width = 0.112 gauss

Table 1: Height and Width values of run 1, run 2, and average for resonance of samples DW, R, S, T, U, H, I, and J

Q	1.00g/100ml	Height = 0.00067 A.U. Width = 0.115 gauss	Height = 0.00049 A.U. Width = 0.177 gauss	Height = 0.00058 A.U. Width = 0.146 gauss

Table 1: Height and Width values of run 1, run 2, and average for resonance of samples M, N, O, P, and Q

These measurements, when input into the graphing software previously used to display the dispersive component of the resonance peaks, leads to the creation of two graphs which present change in height and width as a function of potassium permanganate concentration. These graphs are presented below:

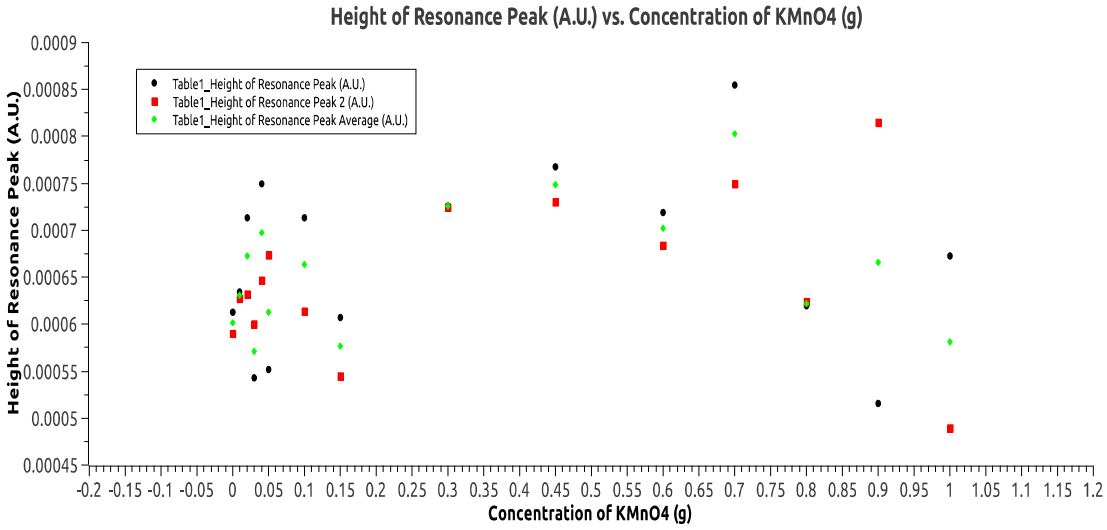

Fig. 53: Height of Resonance Peak (A.U.) vs. Concentration of $KMnO_4$ (g)

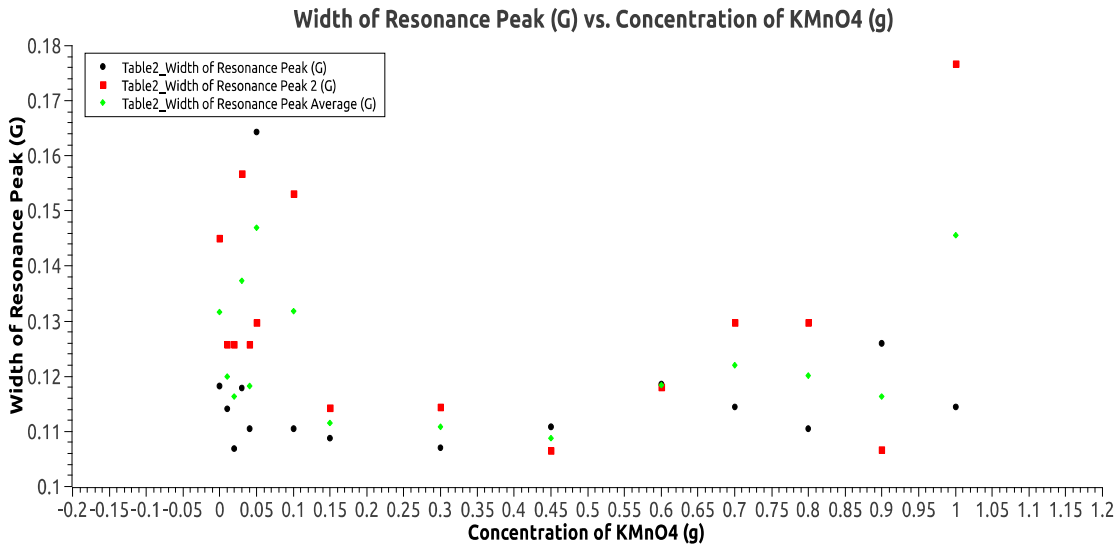

Fig. 54: Width of Resonance Peak (G) vs. Concentration of $KMnO_4$ (g)

Data Analysis

It is observable at low concentrations of $KMnO_4$, that being 0.15g/ml and below, a large amount of noise is apparent in the height and width measurements. This noise is also apparent at higher $KMnO_4$ concentrations, consisting of 0.9 g/ml and above. This noise could arise from a number of sources, such as the two separate runs of the samples being physically placed in different regions of the longitudinal field resulting in the samples experiencing different field inhomogeneities. Another possible source for this noise could be the fact that the Bridged-T circuit was balanced to different degrees for the two separate data runs, which was unfortunately necessary for resonance to be observed on each separate test. Along with these two sources, there is the possibility that the two sample runs were made under different ambient temperature conditions or that the algorithms used to calculate the height and width of the resonance were not as reliable as hoped for these regions of the data.

With this noise issue addressed, one may also be able to observe from these graphs that there is a clear trend in terms of change in height as the concentration increases in the intermediate region between the noisy low and high concentration regions. Initially, the height seems to increase alongside the concentration of potassium permanganate, until reaching a maximum height around the 0.45g to 0.7g range. Once this maximum range is met, the height then begins to decrease as the concentration of potassium permanganate increases, dropping to similar heights as those found at the beginning of the concentration range. This trend in the height is attributed to the fact that, as stated in the saturation theory section, $KMnO_4$ affects that T_1 in a significant manner. This affect takes form in specific ways, such as when low or no concentrations of $KMnO_4$ are present, T_1 is long, meaning that when excited, the nuclei remain in an excited state for relatively long periods of time. This long-excited state period results in suppressed further absorption, as nuclei must be in a lower energy state for absorption to occur. As the $KMnO_4$ concentration increases with each subsequent test the nuclei become more strongly coupled to the lattice and T_1 initially decreases. This initial decrease in the T_1 period then leads to an increased amount of absorption. With the concentration of potassium permanganate constantly increasing with each new test, the value for T_1 eventually becomes so minute that a large amount of the excited nucleons decay to the lower energy state while the magnetic field sweeps across the resonance of the nucleon. This process locks the spin temperature close to the lattice temperature and in doing so suppresses the absorption component. A similar trend of correlation is also observable in the following graph, which depicts the width of the resonance peak as a function of potassium permanganate concentration. However, unlike in the graph for

resonance peak height, the width of the resonance peak seems to slowly but consistently increase as the concentration of potassium permanganate increases. This is easily explained by looking back at the spin-spin part of the background section, which indicates how H_{loc} increases as $KMnO_4$ increases thus causing the width of the resonance peak to increase as well. In short, both the height and width of the resonance peak exhibit clear trends based on the concentration of the potassium permanganate within the sample that align with the previously discussed theoretical understandings of how the compound affects T_1 and T_2. These trends demonstrate that the height of the resonance peak has a well-defined maximum value within a certain range of concentrations, while the width may continue to increase as the concentration of the compound increases.

Error Analysis

For any research performed through an experimental system, there are a number of sources of error that occur over the course of the experimentation process. This understanding does not fail to apply to this research project in particular, as throughout the course of the performing the experiments, several possible forms of error arose and should be accounted for while discussing the results. The first of these possible sources of error arises from the placement in elevation of the sample holder. The sample holder, while created specifically for this experimental NMR system, was most likely not at the exact middle vertical point of the magnets that make-up the inner magnet system. The result of this approximated placement then indicates that any sample placed inside the sample holder may not have been in the exact middle of the magnet system either. Should this be the case, then therein lies the very real possibility that the magnetic field

created by the magnet would have produced a field inhomogeneity across the sample, meaning that the magnetic field could have affected some parts of the $KMnO_4$ samples to a different degree than other parts of the sample. There even may be observable evidence of this fluctuation, as one should also note the erratic behavior exhibited in the smallest potassium permanganate concentrations, that being from 0.0g to 0.1g. This inconsistent performance displayed in this part of the data is possible due to the fact that, at lower concentrations, the inhomogeneities that would occur from where the sample is placed in the experimental NMR system would be more pronounced, and thus are easier to see through the results of the experiments. Ultimately, the placement of the sample within the system plays a significant role in the accuracy of the system and given the experimental aspects of this system in particular, possible sources of error must be given consideration. The next possible source of error comes in the form of the wiring that connected many components of the experimental NMR system, that being primarily BNC cable. These cables, while standard for many of the equipment, could be temperamental, as too much movement of said wires while the machine is running could cause certain measurements on the oscilloscope to change. Obviously, the solution to this issue was to simply limit any and all movement of the wires while the system was in use, but such fluctuations must be noted for the sake of interpretation in regard to the resulting data.

Finally, the last obvious source of possible error arises from the issue of temperature fluctuations within the air and their adverse effects on the circuit board and the wiring which connects the board and the sample holder. While some forms of temperature shielding were implemented in the form of a Teflon tube and aluminum

box to offer some passive temperature control against fluctuations, these components did not offer any form of active temperature control that would allow the temperature inside the magnet to be completely constant while experiments were being performed. Furthermore, due to having to be capable of moving the Teflon tube in and out of place to switch samples, the area between the tube and the aluminum box was not air tight, thus limiting the level of control that could be implemented using passive means. Ultimately, while the passive temperature control did help with the process of gaining more stability with the NMR system, it did not entirely eliminate the problem, only restricted the effects.

Conclusion

While the process by which the data was attained presented possible sources of error and complications, ultimately the results were consistent with the theory previously expressed. The $KMnO_4$ added to the deionized water within the samples should have, theoretically, initially increased the rate of absorption within the nuclei by increasing the spin-lattice coupling and thus decreasing the T_1 value. This decrease in the T_1 value would then lead to the height of the resonance peak to increase, as the height designates how much or how little absorption is occurring. Conversely, the added $KMnO_4$ should have also caused the T_1 value to become small enough at higher concentrations of the compound that it starts to lock the spin temperature close to the lattice temperature, thus causing the absorption and the height of the resonance peak to decrease. The finalized results demonstrated this, as the height of the resonance increases to a maximum value and then decreases as the concentration of $KMnO_4$ continues to increase. Ultimately, the data exhibits the general behavior that was previously outlined in the theory section of this paper, and thus confirms the findings to be consistent with the theory previously stated.

Ultimately, one must ask again why these findings are relevant, and why the use of nuclear magnetic resonance spectroscopy is important to the field of physics overall. This thesis, while examining a compound that has been analyzed before, does so with a unique purpose, that being gauging how concentration of $KMnO_4$ plays a role in NMR of protons. Through this one learns that the concentration can affect the size of the resonance peak observed through the oscilloscope and overall how much coupling occurs in regard to compounds being experimented on through NMR spectroscopy.

These findings also indicate the possible benefits of the application of potassium permanganate to other compounds. By applying certain amounts of potassium permanganate to other materials, one could potentially increase the observability of the resonance peak when said materials are analyzed with an NMR spectrometer. While not absolutely revolutionary, in science, physics especially, it is important to examine all avenues of study and take note of every detail. Someday, this research may play a part in another budding physicists' own interest into the field of nuclear magnetic resonance, and through that interaction the ever-growing cycle of scientific interest continues onward, spawning more and more development in both the field of NMR and in physics as a whole.

List of Variables

- H_0 = steady magnetic field, longitudinal field
- I = spin number
- μ = magnetic moment
- h bar = reduced Planck constant
- E = energy
- ω_0 = Larmor frequency
- γ = gyromagnetic ratio
- T_s = equilibrium temperature, temperature at which nuclear spins are in equilibrium, spin temperature
- T = lattice temperature
- T_1 = spin-lattice relaxation time
- W = average transition rate between upward transition and downward transition
- H_{loc} = adjacent local magnetic field
- H_{tot} = total magnetic field
- μ_0 = magnetic dipole moment of one nucleus
- g = g-factor
- T_2 = spin-spin relaxation time
- $g(\nu)_{max}$ = maximum value of line-shape function as a function of ν
- n = excess nuclei in lower energy state
- n_0 = excess number of nuclei in lower energy state when spin system and lattice are in thermal equilibrium

- $\frac{dn}{dt}$ = rate of change in excess number of nuclei in lower energy state as function of time
- P = probability per unit time that a nuclei transitions to a higher energy state
- n_s = steady state of n
- Z = saturation factor

Bibliography

Andrew, E. Raymond. Nuclear Magnetic Resonance. University Press, 1958.

Balti, Metin. “Resonance Phenomena-2.” *Basic 1H- and 13C-NMR Spectroscopy*, 2005, pp. 9–24.

Becker, E D. “A Brief History of Nuclear Magnetic Resonance.” *Analytical Chemistry*, vol. 65, no. 6, 1993, pp. 295A–302A.

Broze, M., and Z. Luz. “Oxygen-17 Spin-Spincoupling with Manganese-55 and Carbon-13.” *The Journal of Physical Chemistry*, vol. 73, no. 5, 1969, pp. 1600–1602.

Callaghan, P.T. “Nuclear Magnetic Resonance.” *Encyclopedia of Mathematical Physics*, pp. 592–600.

Foroozandeh, Mohammadali, et al. “Ultrahigh-Resolution Total Correlation NMR Spectroscopy.” *Journal of the American Chemical Society*, vol. 136, no. 34, 2014, pp. 11867–11869.

Gudlin, D, and H Schneider. “Manganese-55 Nuclear Magnetic Resonance Studies of Potassium Permanganate Solutions at 22°C.” *Journal of Magnetic Resonance* (1969), vol. 17, no. 2, 1975, pp. 268–271.

Pfeifer, H. “A Short History of Nuclear Magnetic Resonance Spectroscopy and of Its Early Years in Germany.” *Magnetic Resonance In Chemistry*, vol. 37, 1999, pp. S154–S159.

Soderberg, Tim, and Open Textbook Library, distributor. *Organic Chemistry with a Biological Emphasis. Volume I, Chapters 1-8*. University of Minnesota Morris, 2016.

Waring, Charles E., et al. “A Bridged Tee Detector for Nuclear Magnetic Resonance.” *Review of Scientific Instruments*, vol. 23, no. 9, 1952, pp. 497–498.

Wadsworth, M, and P.W France. “NMR Dispersive Mode Resonance of 55Mn in Polycrystalline KMnO 4.” *Journal of Magnetic Resonance* (1969), vol. 51, no. 3, 1983, pp. 424–429.